

Effective rigidity of neutron monitor: new method of the solar energetic particle fluence assessing using neutron monitor data

Sergey Koldobskiy

Oulu University, Oulu, Finland and National Research
Nuclear University, Moscow, Russia

Alexandar Mishev, Gennady Kovaltsov,
Ilya Usoskin

Based on:

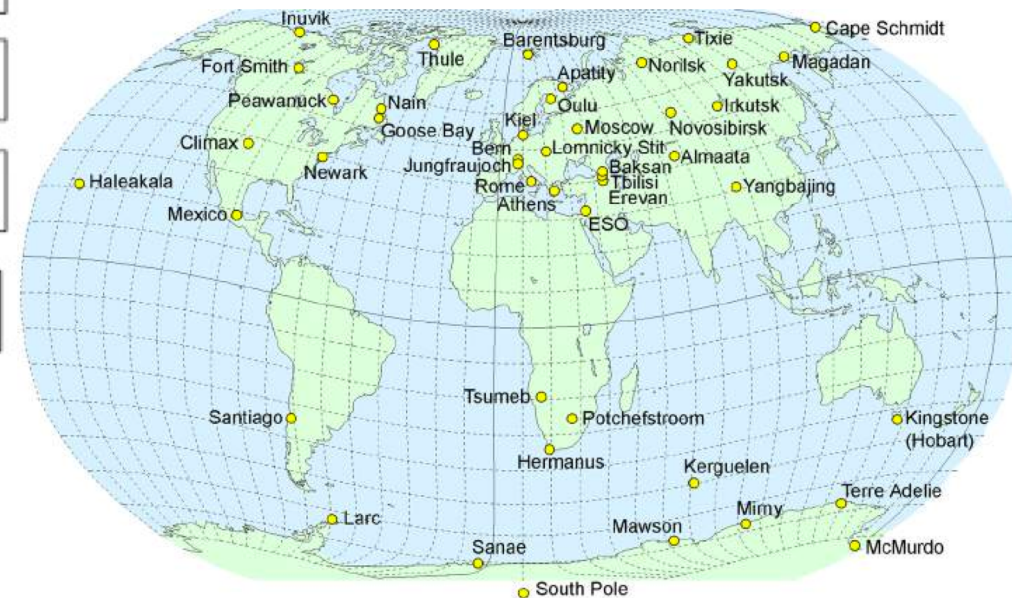
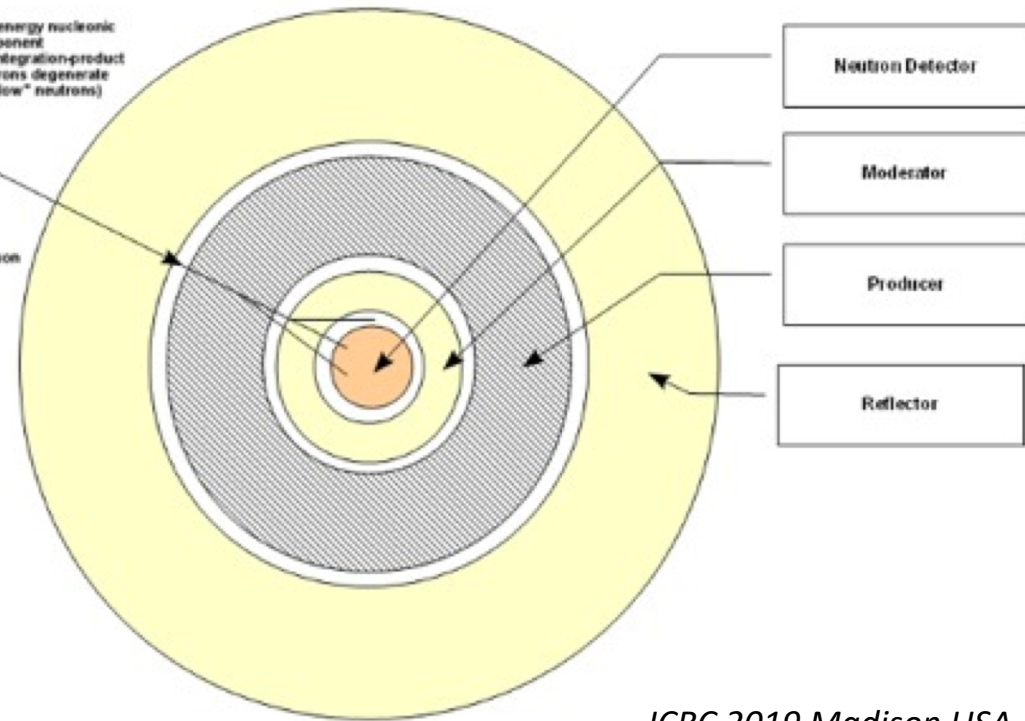
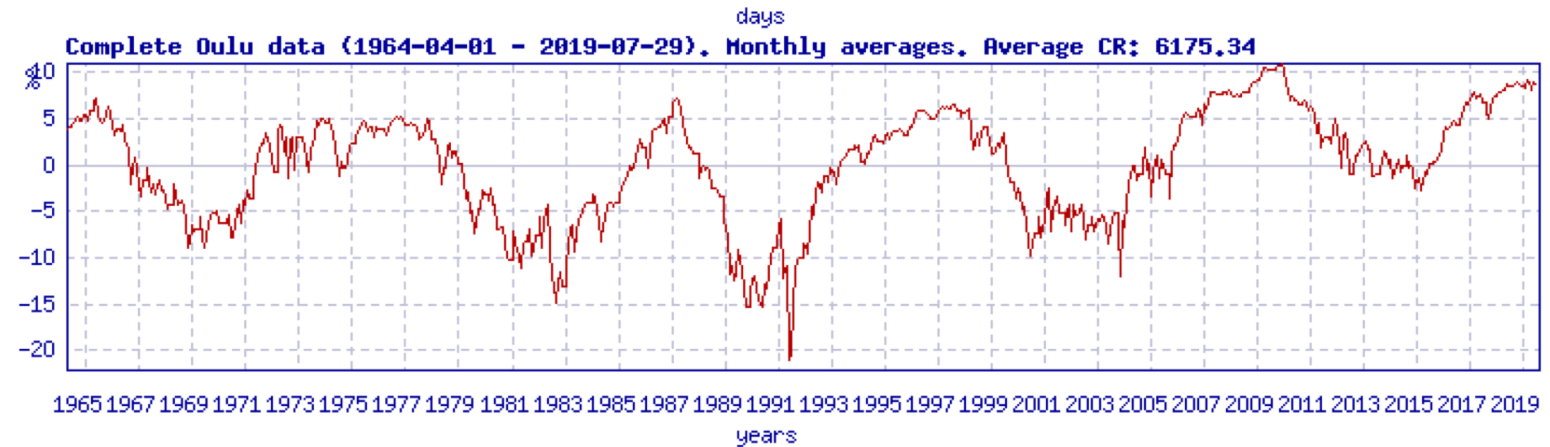
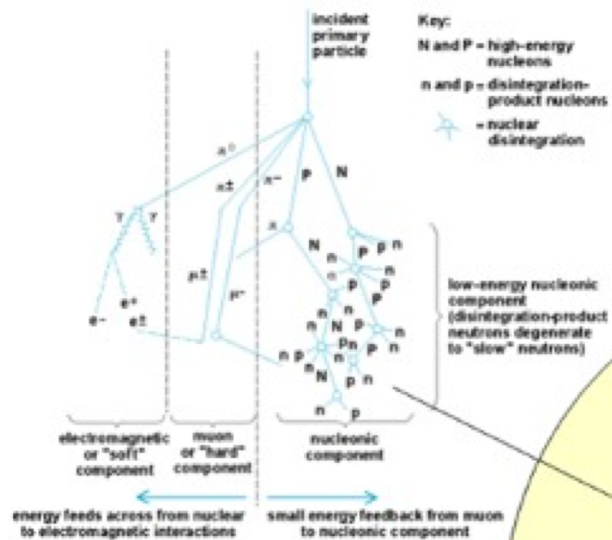
Solar Physics (2018) 293:110

Solar Physics (2019) 294:94

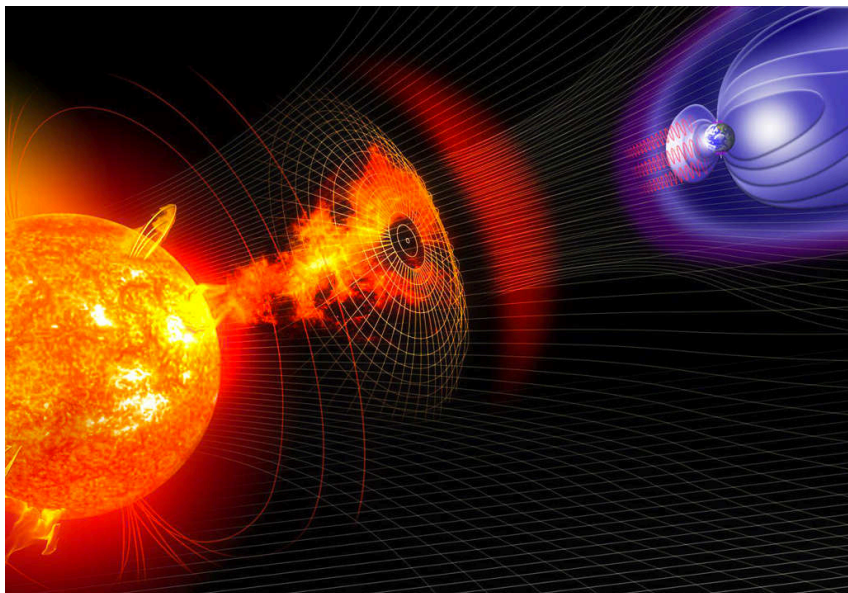
Outline

1. Motivation.
2. The new R_{eff} method.
3. Reconstruction of SEP fluence for GLE #69 and 71 using R_{eff} method.
4. Conclusion

Neutron Monitors

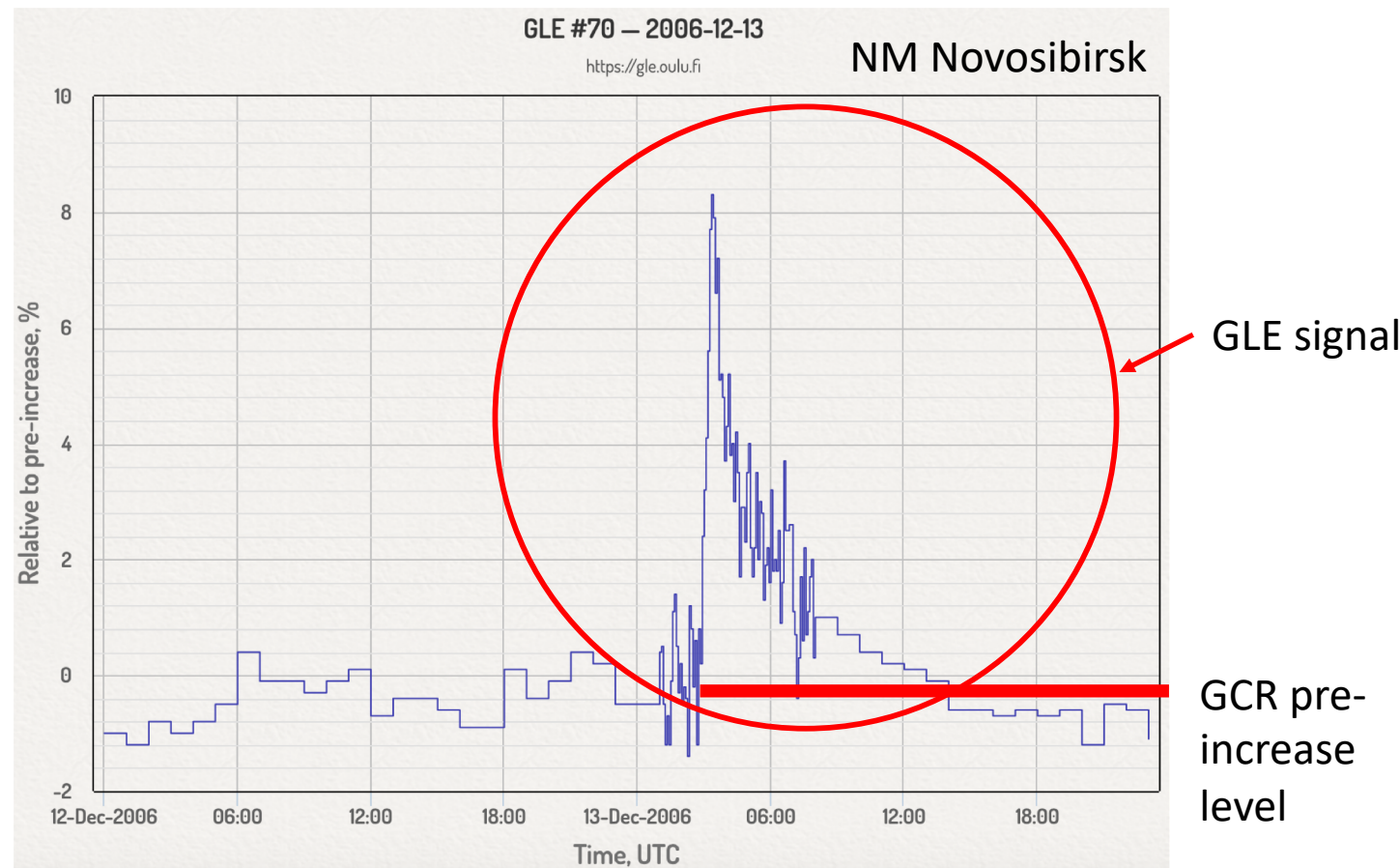


GLE integral increase



From the GLE database (gle.oulu.fi) we have calculated relative integral increases from SEP during GLE events in the units of relative units of [% * hour]

$$N_{\text{GLE}} = X * N_{\text{GCR}}$$



Overview on recent results

PROCEEDINGS OF THE 31st ICRC, LODZ 2009

A New and Comprehensive Analysis of Proton Spectra in Ground-Level Enhanced (GLE) Solar Particle Events

Allan J. Tylka* and William F. Dietrich^{†*}

J. Space Weather Space Clim. 2018, 8, A04
© O. Raukunen et al., Published by EDP Sciences 2018
<https://doi.org/10.1051/swsc/2017031>



Available online at:
www.swsc-journal.org

Measurement, Specification and Forecasting of the Solar Energetic Particle Environment and GLEs

RESEARCH ARTICLE

OPEN ACCESS

Two solar proton fluence models based on ground level enhancement observations

Osku Raukunen^{1,*}, Rami Vainio¹, Allan J. Tylka², William F. Dietrich³, Piers Jiggins⁴, Daniel Heynderickx⁵, Mark Dierckxsens⁶, Norma Crosby⁶, Urs Ganse⁷ and Robert Siipola¹

The Band function:

$$J(>R) = \begin{cases} J_0 \left(\frac{R}{1 \text{ GV}} \right)^{-\gamma_1} \exp \left(-\frac{R}{R_0} \right), & R < (\gamma_2 - \gamma_1) R_0 \equiv R_1 \\ J_0 \left(\frac{R_1}{1 \text{ GV}} \right)^{-\gamma_1} \exp \left(-\frac{R_1}{R_0} \right) \left(\frac{R}{R_1} \right)^{-\gamma_2}, & R \geq R_1 \end{cases} \quad (1)$$

Here $J(>R)$ is the omnidirectional event-integrated integral fluence in units of cm^{-2} , J_0 is an overall fluence normalization coefficient, γ_1 is the low rigidity power law index, γ_2 the high rigidity power law index and $(\gamma_2 - \gamma_1)R_0 \equiv R_1$ is the breakpoint rigidity. The Band function is constructed in such a way that both the function and its first derivative are continuous.

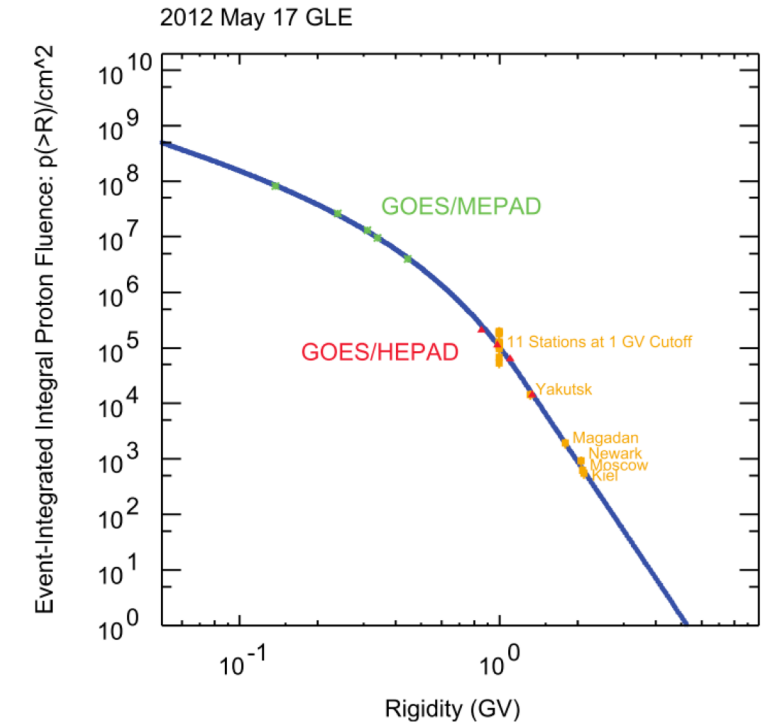


Fig. 1. Event-integrated proton fluence spectrum for GLE 71. NM observations are shown in orange, GOES/MEPAD in green, GOES/HEPAD in red and the Band-fit spectrum in blue.

Table 2. Spectral parameters of GLEs and their ESP counterparts. The uncertainties are estimated by varying the parameter of interest while holding the other parameters at their best-fit values.

GLE	Episode	J_0 (p/cm ²)	ΔJ_0 (p/cm ²)	γ_1	$\Delta \gamma_1$	γ_2	$\Delta \gamma_2$	R_0 (GV)	ΔR_0 (GV)
5	1	1.75E+08	1.59E+07	1.76	0.06	5.04	0.12	5.66E-01	3.49E-02
7	3	7.88E+08	7.96E+07	1.35	0.08	6.08	0.22	1.44E-01	5.50E-03
8	4	8.16E+05	9.42E+04	1.53	0.08	4.88	0.17	5.85E-01	3.93E-02
9	5	1.24E+08	1.36E+07	0.32	0.08	5.56	0.35	1.41E-01	5.70E-03
10	6	1.22E+08	1.41E+07	2.76	0.09	6.54	0.14	3.47E-01	1.97E-02
11	6	3.33E+07	4.11E+06	3.14	0.09	7.00	0.11	4.38E-01	2.84E-02

Why are we decided to update calculations?

1. Method uses prescribed function and finds the best-fit parameters for it. What if is prescribed function is wrong? → **Create the method of fluence assessment independent from the prescribed SEP function.**
2. Reconstruction uses neutron monitor yield function by Clem and Dorman (SSR, 2000). Neutron monitor yield function validation using AMS-02 data showed that this yield function possibly overestimates the low-energy particles response in neutron monitor together with Ma16 yield function and Mi13 and CM12 shows better performance during validation. → **Use Mi13 yield function**

The R_{eff} method

Let me start from definition:

The “effective” rigidity of a neutron monitor for a ground-level enhancement (GLE) event is defined so that the event-integrated fluence of solar energetic protons with rigidity above it is directly proportional to the integral intensity of the GLE as recorded by a polar neutron monitor, within a wide range of solar energetic-proton spectra.

Solar Phys (2018) 293:110
<https://doi.org/10.1007/s11207-018-1326-1>

Effective Rigidity of a Polar Neutron Monitor for Recording Ground-Level Enhancements

Sergey A. Koldobskiy^{1,2}  · Gennady A. Kovaltsov³  ·
Ilya G. Usoskin^{1,4} 



$$F(>R_{\text{eff}}) = K_{\text{eff}} N_{\text{GLE}},$$

where K_{eff} is (nearly) constant in the entire range of realistic GLE proton spectra and N_{GLE} is an integral NM response to GLE protons.

Theoretical NM response can be calculated as:

$$N(P_c, h) = \sum_j \int_{P_c}^{\infty} J_j(R) \cdot Y_j(R, h) \cdot dR,$$

where $Y_j(R, h)$ is the yield function of the NM (located at height h) for primary cosmic-ray particles of type j (protons, helium, heavier species), and J_j is the differential intensity of primary particles of type j at the Earth's orbit

Here we used NM yield function by Mishev et al. (2013) with altitudinal dependence from Fluckiger et al. (2008)

The R_{eff} method

$K_{\text{eff}} = F(>R_{\text{eff}}) / N_{\text{GLE}}$ and K_{eff} for given R must be constant irrespectively from the SEP fluence function

First we have tested this method using simple power-law:

$$F(>R) = F_0 R^{-\gamma}$$

and

$$K_{\text{eff}}(R) = \frac{F(>R)}{\int_{P_c}^{\infty} \frac{dF(R)}{dR} Y(R) dR}$$

The R_{eff} method

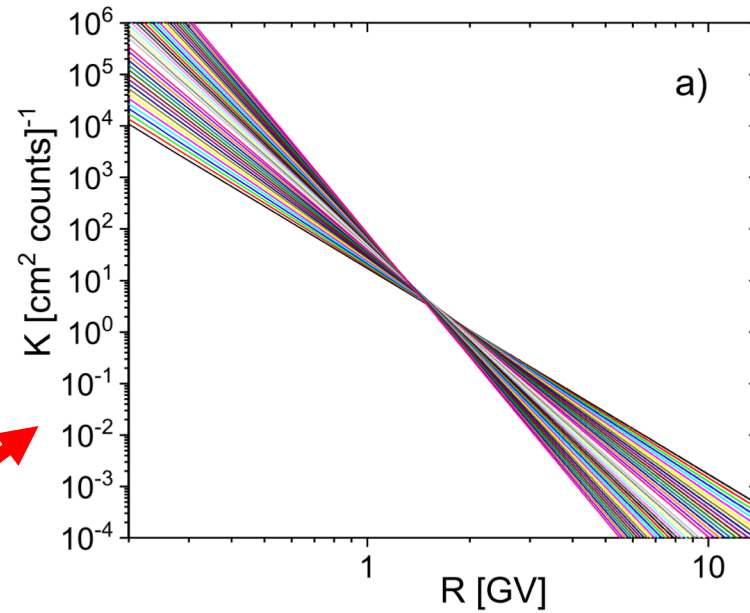
$K_{\text{eff}} = F(>R_{\text{eff}}) / N_{\text{GLE}}$ and K_{eff} for given R must be constant irrespectively from the SEP fluence function

First we have tested this method using simple power-law:

$$F(>R) = F_0 R^{-\gamma}$$

and

$$K_{\text{eff}}(R) = \frac{F(>R)}{\int_{P_c}^{\infty} \frac{dF(R)}{dR} Y(R) dR}$$



The R_{eff} method

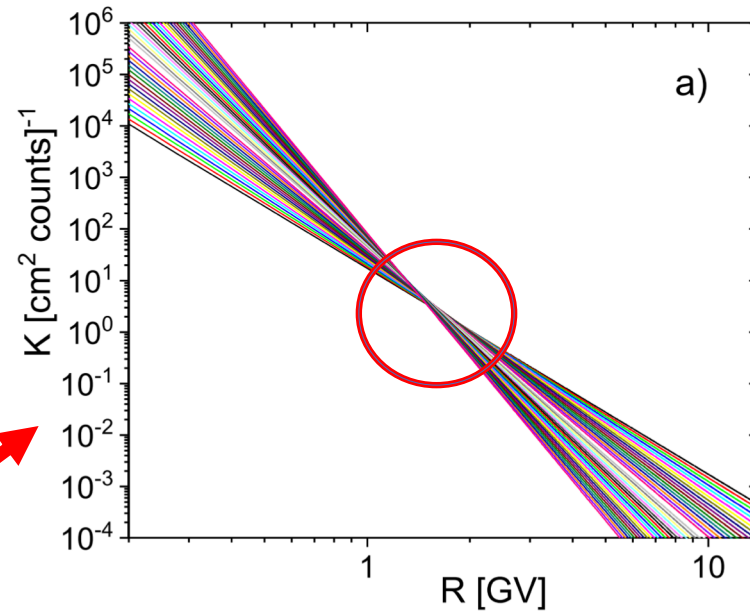
$K_{\text{eff}} = F(>R_{\text{eff}}) / N_{\text{GLE}}$ and K_{eff} for given R must be constant irrespectively from the SEP fluence function

First we have tested this method using simple power-law:

$$F(>R) = F_0 R^{-\gamma}$$

and

$$K_{\text{eff}}(R) = \frac{F(>R)}{\int_{P_c}^{\infty} \frac{dF(R)}{dR} Y(R) dR}$$



The R_{eff} method

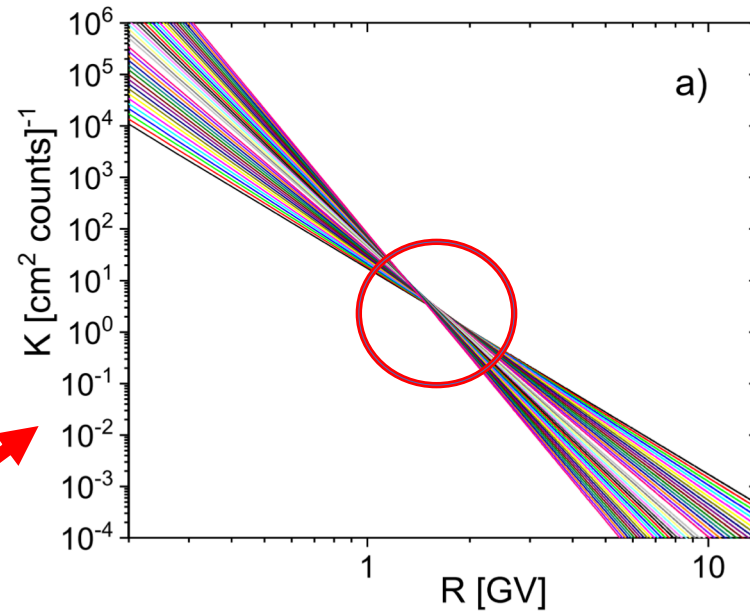
$K_{\text{eff}} = F(>R_{\text{eff}}) / N_{\text{GLE}}$ and K_{eff} for given R must be constant irrespectively from the SEP fluence function

First we have tested this method using simple power-law:

$$F(>R) = F_0 R^{-\gamma}$$

and

$$K_{\text{eff}}(R) = \frac{F(>R)}{\int_{P_c}^{\infty} \frac{dF(R)}{dR} Y(R) dR}$$



After that we moved to Band functions from Raukunen et al. 2018:

$$F(>R) = \begin{cases} J_0 \left(\frac{R}{1\text{GV}} \right)^{-\gamma_1} \exp\left(-\frac{R}{R_0}\right), & R < (\gamma_2 - \gamma_1)R_0 \equiv R_1 \\ J_0 \left(\frac{R_1}{1\text{GV}} \right)^{-\gamma_1} \exp\left(-\frac{R_1}{R_0}\right) \left(\frac{R}{R_1} \right)^{-\gamma_2}, & R \geq R_1 \end{cases}$$

The R_{eff} method

$K_{\text{eff}} = F(>R_{\text{eff}}) / N_{\text{GLE}}$ and K_{eff} for given R must be constant irrespectively from the SEP fluence function

First we have tested this method using simple power-law:

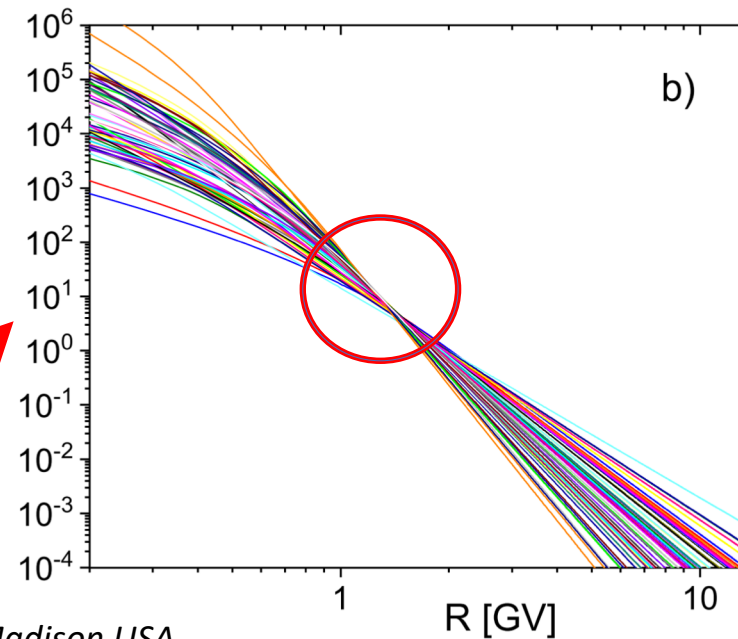
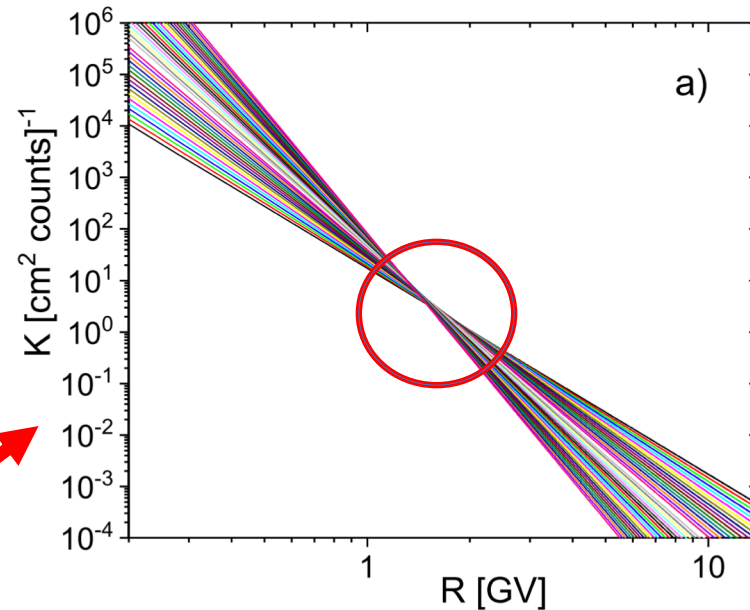
$$F(>R) = F_0 R^{-\gamma}$$

and

$$K_{\text{eff}}(R) = \frac{F(>R)}{\int_{P_c}^{\infty} \frac{dF(R)}{dR} Y(R) dR}$$

After that we moved to Band functions from Raukunen et al. 2018:

$$F(>R) = \begin{cases} J_0 \left(\frac{R}{1 \text{ GV}} \right)^{-\gamma_1} \exp\left(-\frac{R}{R_0}\right), & R < (\gamma_2 - \gamma_1) R_0 \equiv R_1 \\ J_0 \left(\frac{R_1}{1 \text{ GV}} \right)^{-\gamma_1} \exp\left(-\frac{R_1}{R_0}\right) \left(\frac{R}{R_1} \right)^{-\gamma_2}, & R \geq R_1 \end{cases}$$



The R_{eff} method

$K_{\text{eff}} = F(>R_{\text{eff}}) / N_{\text{GLE}}$ and K_{eff} for given R must be constant irrespectively from the SEP fluence function

First we have tested this method using simple power-law:

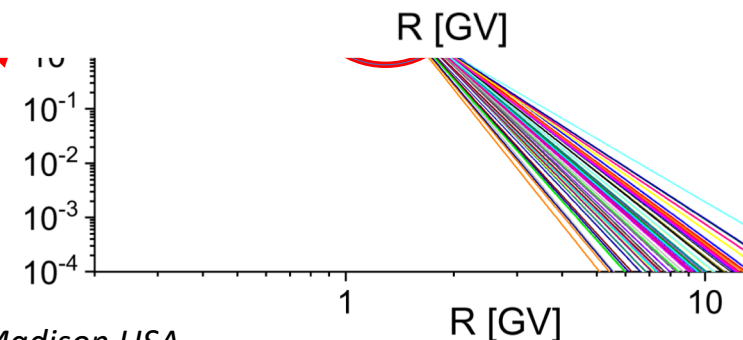
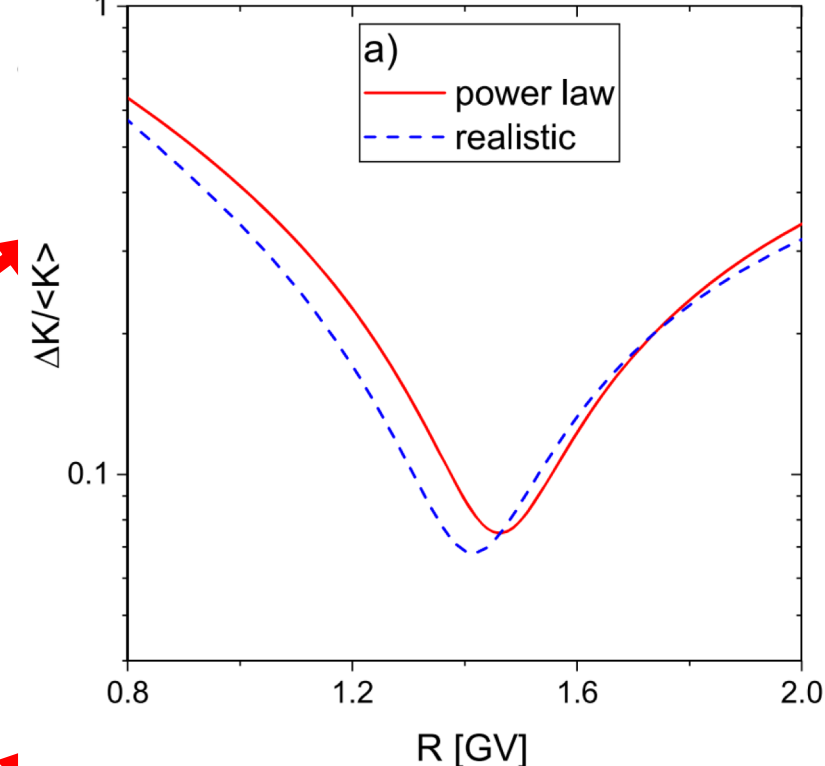
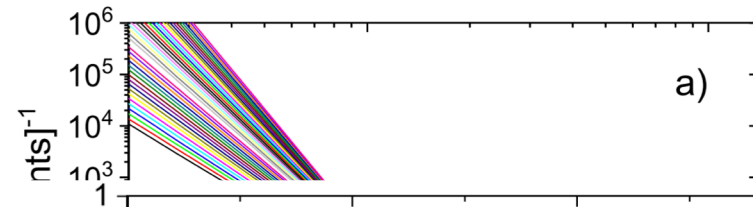
$$F(>R) = F_0 R^{-\gamma}$$

and

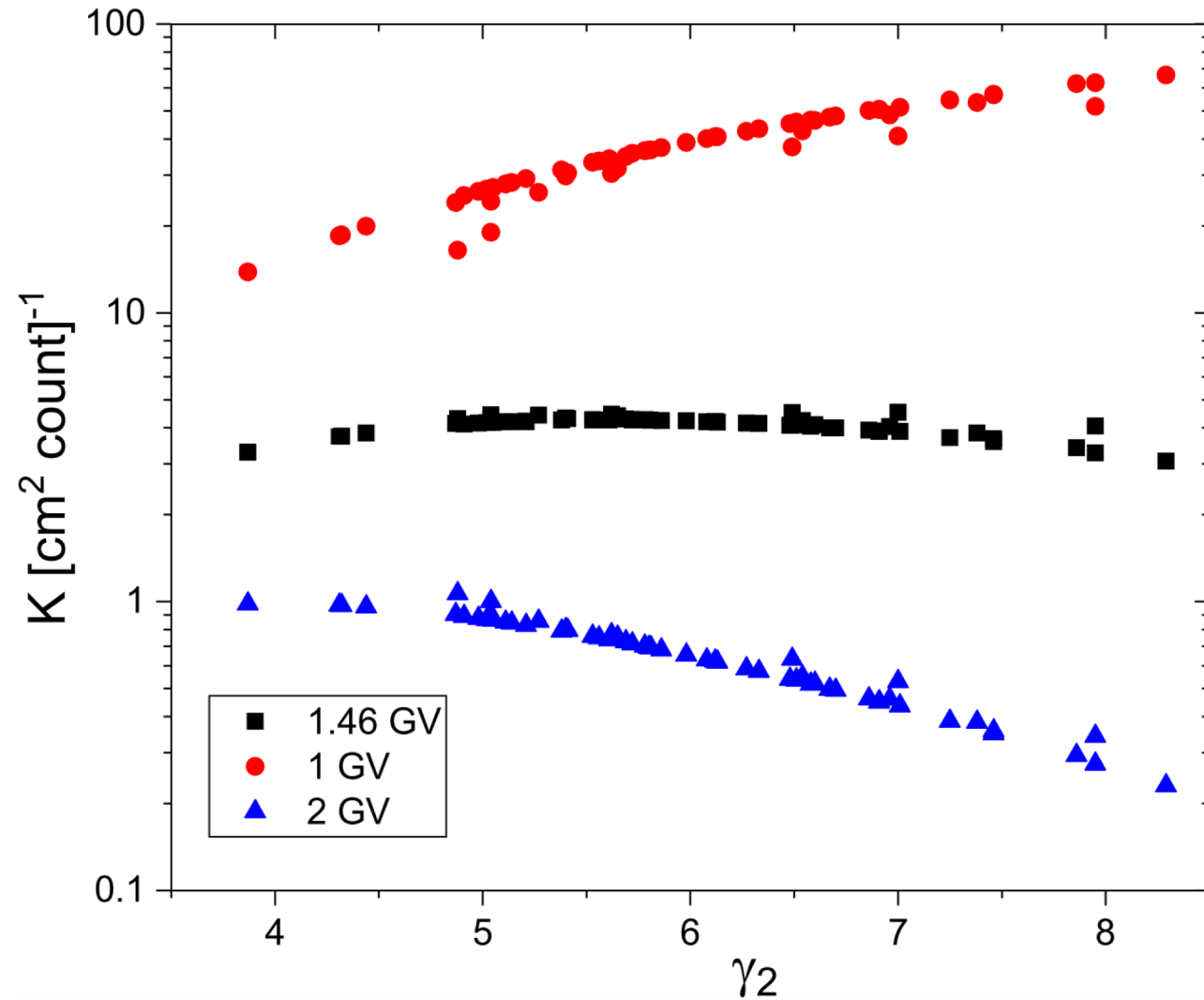
$$K_{\text{eff}}(R) = \frac{F(>R)}{\int_{P_c}^{\infty} \frac{dF(R)}{dR} Y(R) dR}$$

After that we moved to Band functions from Raukunen et al. 2018:

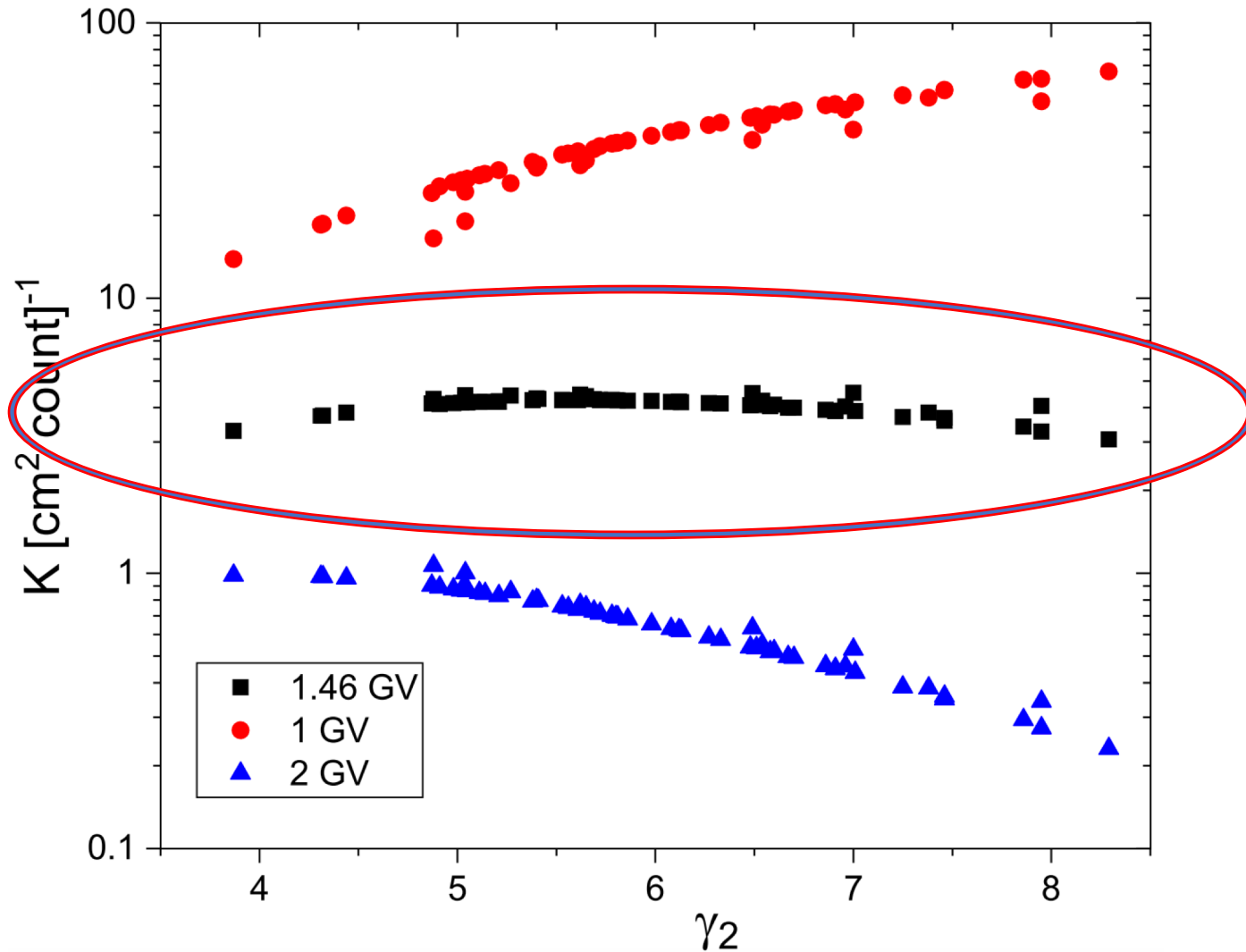
$$F(>R) = \begin{cases} J_0 \left(\frac{R}{1 \text{ GV}} \right)^{-\gamma_1} \exp\left(-\frac{R}{R_0}\right), & R < (\gamma_2 - \gamma_1) R_0 \equiv R_1 \\ J_0 \left(\frac{R_1}{1 \text{ GV}} \right)^{-\gamma_1} \exp\left(-\frac{R_1}{R_0}\right) \left(\frac{R}{R_1} \right)^{-\gamma_2}, & R \geq R_1 \end{cases}$$



The R_{eff} method



The R_{eff} method



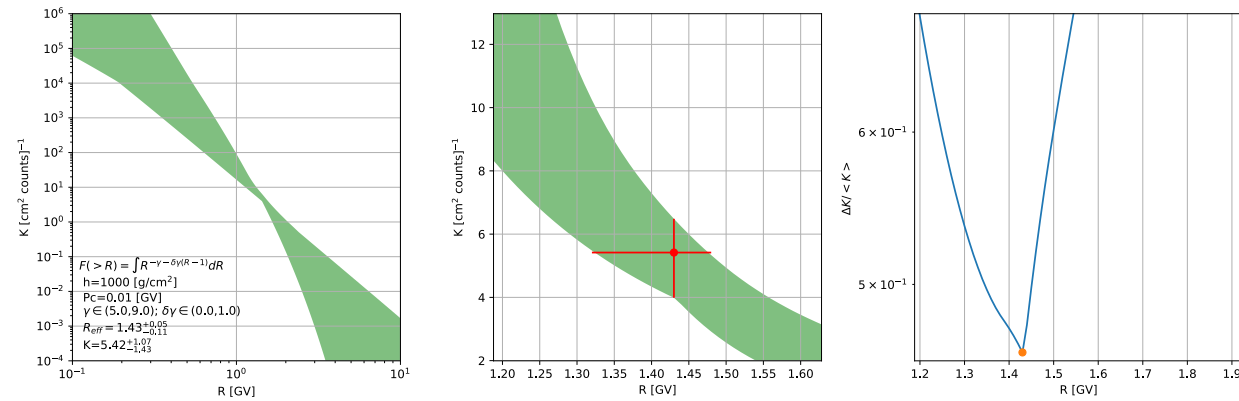
K is not depended from γ if we will use the effective value of rigidity

Therefore, the effective rigidity approach works!

Next we considered the modified power law in rigidity

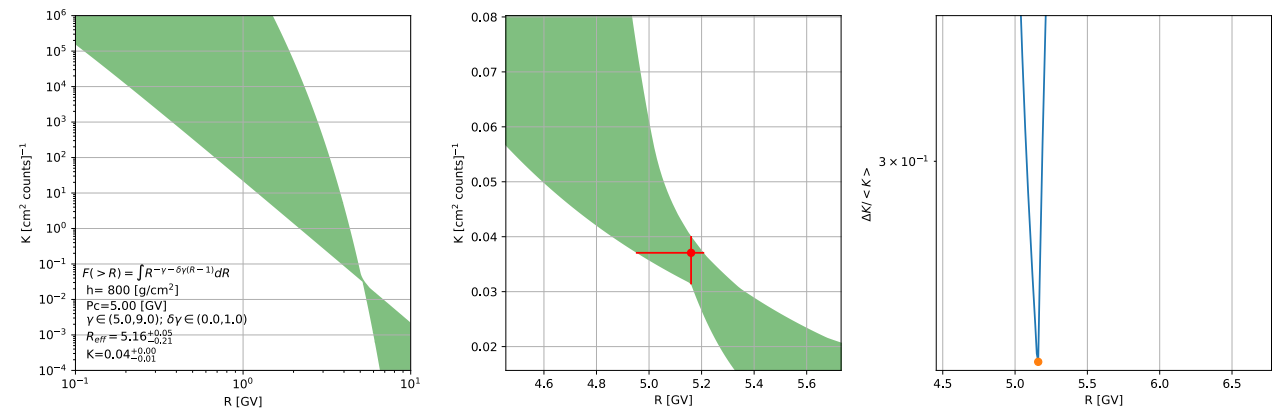
$$\frac{dF}{dR} = F_0 R^{-(\gamma + \delta\gamma(R-1))} \quad ; \quad \text{and varied the } \delta\gamma \text{ from 0 (no steeping) to 1 (strong steeping)}$$

$P_c=0$ GV, $h=1000$ g/cm²

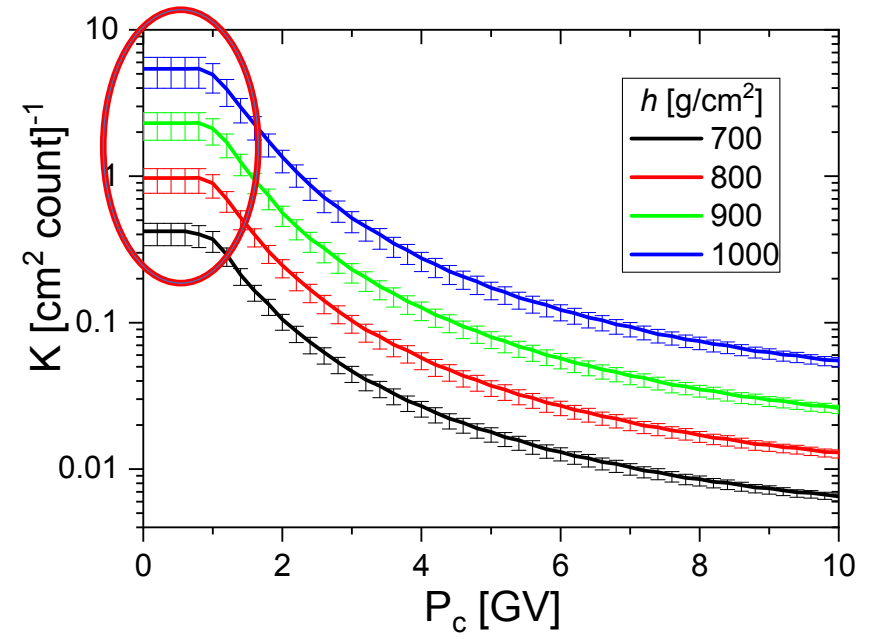
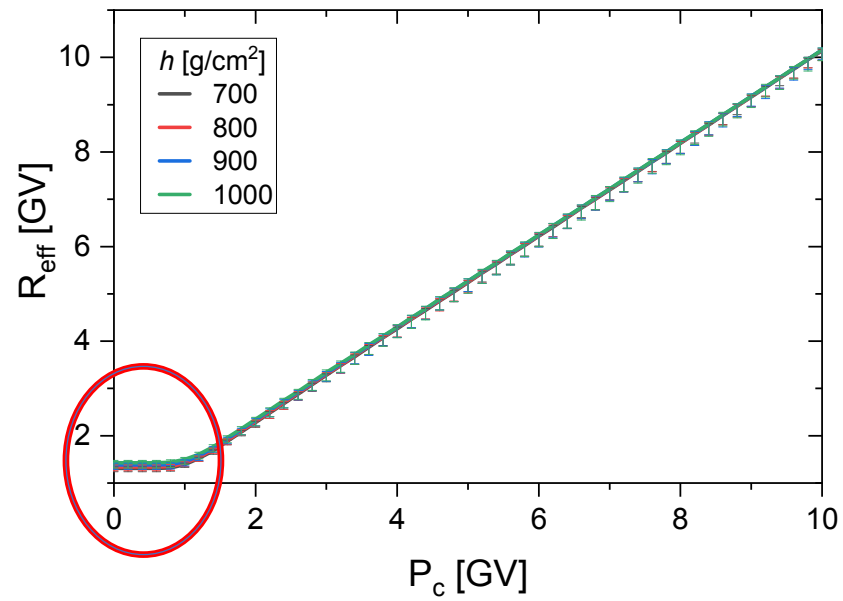


Next we have moved to consideration of different attitudes and cutoff rigidities, using altitudinal dependence from Fluckiger et al. (2008)

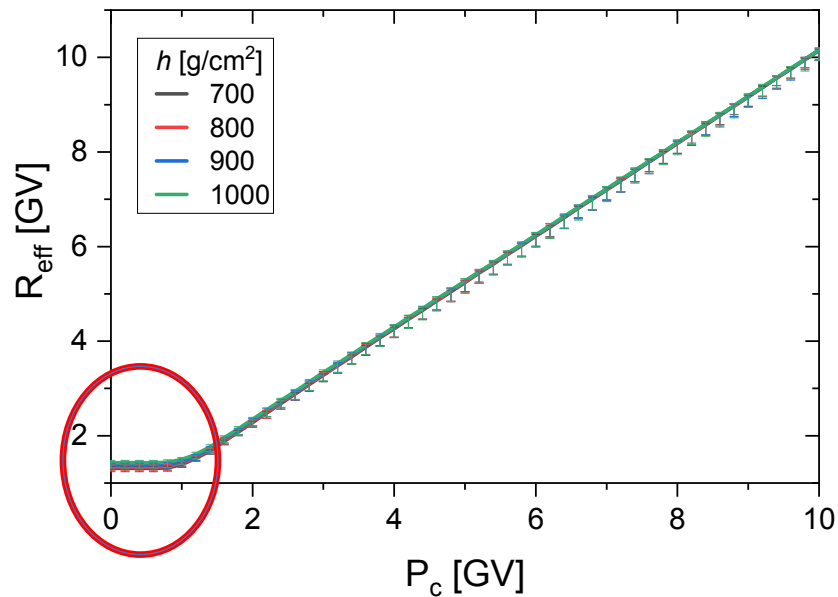
$P_c=5$ GV, $h=800$ g/cm²



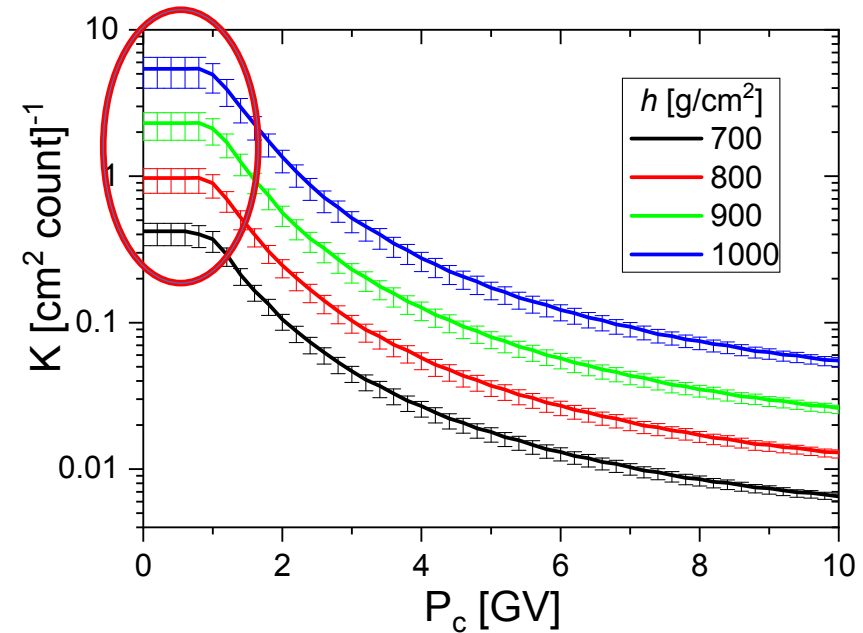
R_{eff} and K_{eff} as functions of P_c and h



R_{eff} and K_{eff} as functions of P_c and h



Effective rigidity R_{eff} is very close to the geomagnetic rigidity cutoff P_c for low- and mid-latitude locations ($P_c > 3$ GV) but saturates at 1.3–1.5 GV (depending on the atmospheric depth) for high-latitude sites.



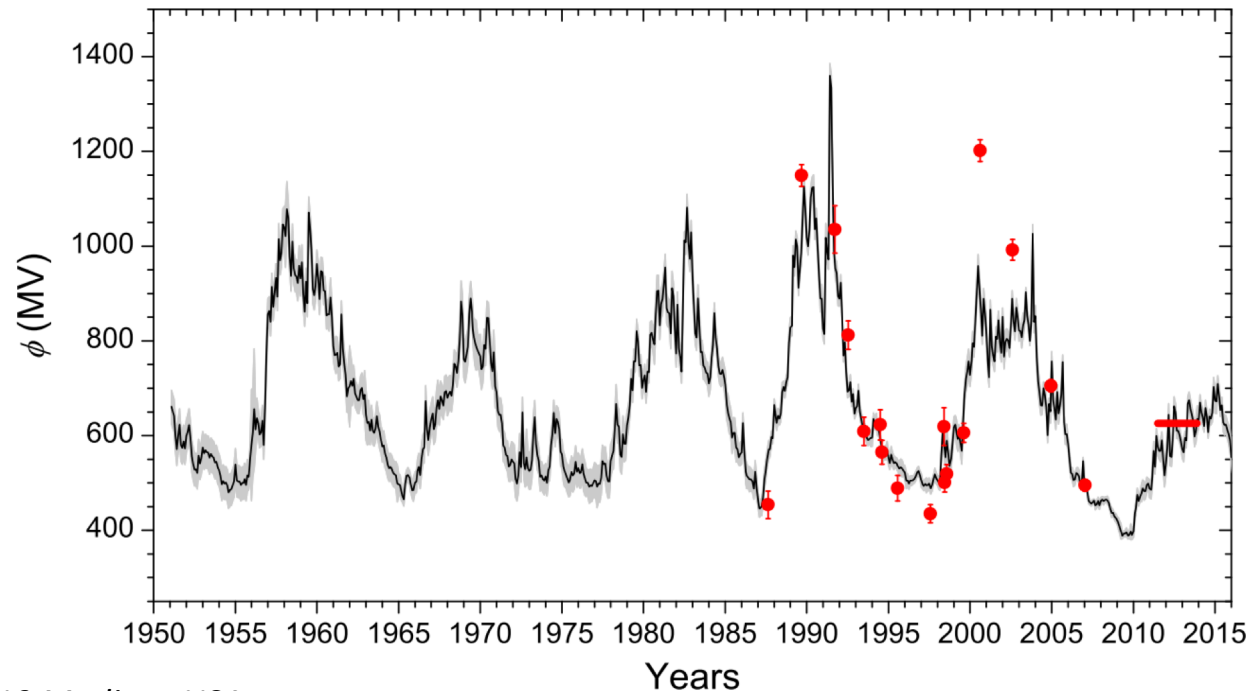
The value of the K_{eff} varies with the geomagnetic cutoff depicting a shoulder at high-latitude locations and a nearly exponential decrease with P_c for low- and mid-latitudes.

These relations are shaped by two different processes, viz. the atmospheric cutoff (particles must possess sufficient energy of a several hundred MeV to initiate an atmospheric cascade reaching the ground) and the geomagnetic cutoff (particles must possess sufficient rigidity to be able to enter the atmosphere). While the geomagnetic cutoff dominates at low- and mid-latitudes, the atmospheric cutoff becomes crucial at high latitudes.

Galactic cosmic ray background

In order to assess GCR spectrum during GLEs, we used:

- Smart and Shea P_c
- Simplified solar modulation model by Axford and Gleeson 1968
- Modern LIS by Vos & Porgieter 2015, verified with both PAMELA and AMS-02 data (Koldobskiy et al. 2019)
- ϕ values were taken from Usoskin et al. 2017



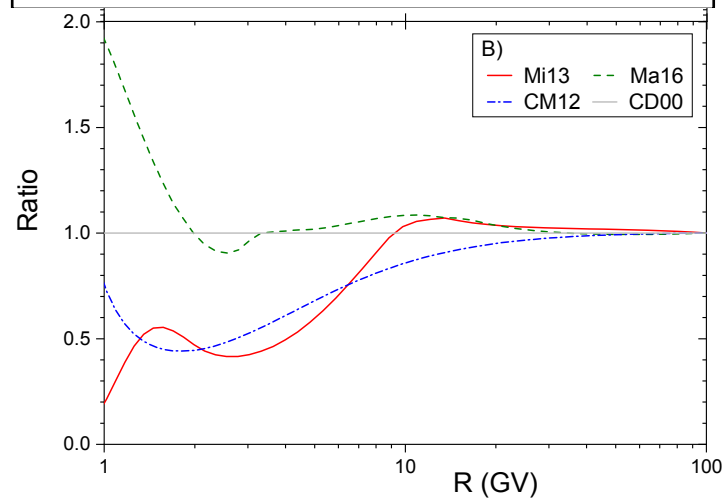
Test

Now we have everything to reconstruct the SEP fluence with point-by-point structure with the new method

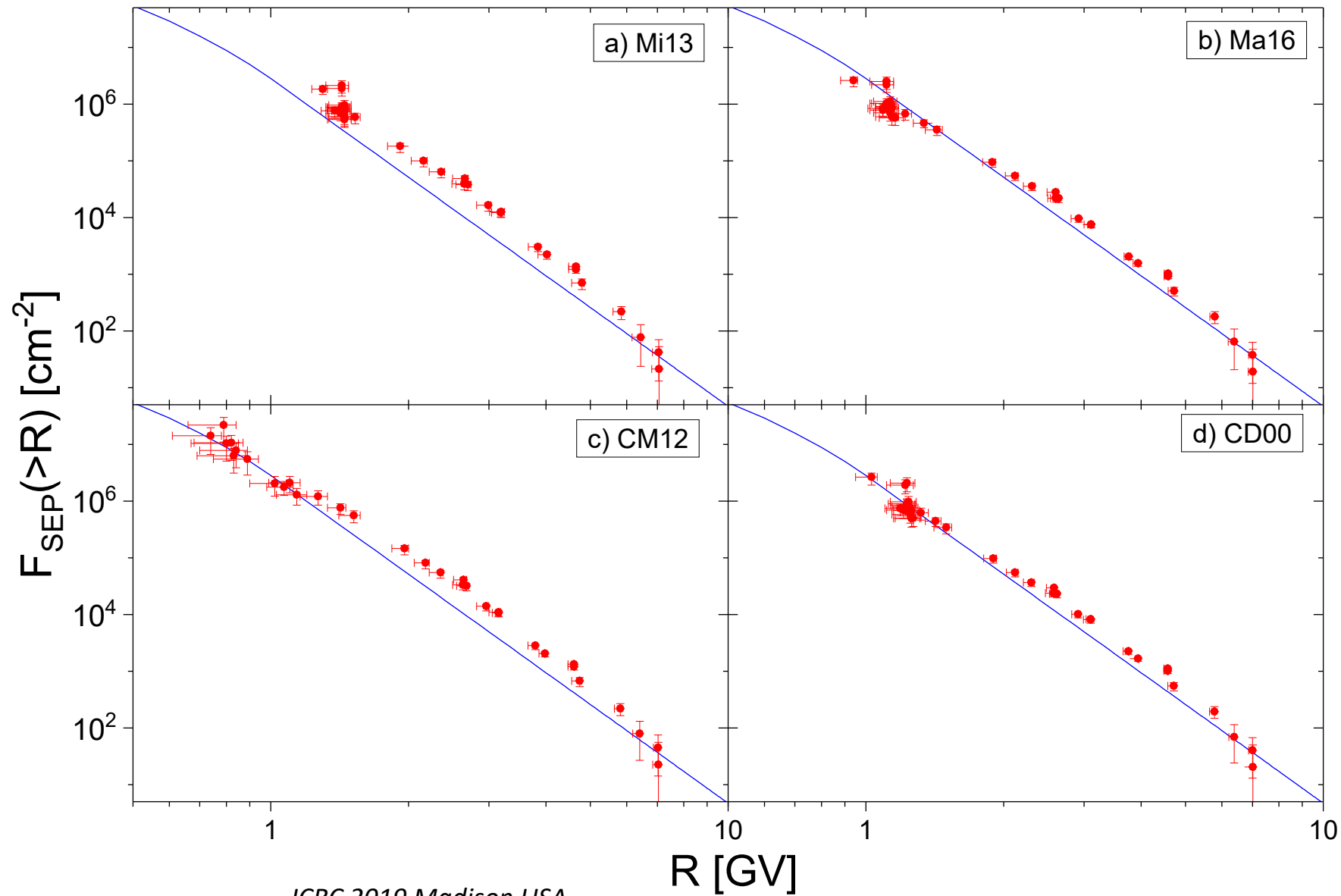
Four modern neutron monitor yield function were tested:

- Mishev et al. 2013
- Caballero-Lopez and Moraal 2012
- Mangeard et al. 2016
- Chem and Dorman 2000

For all these YFs the attitude dependence from FI08 YF was used



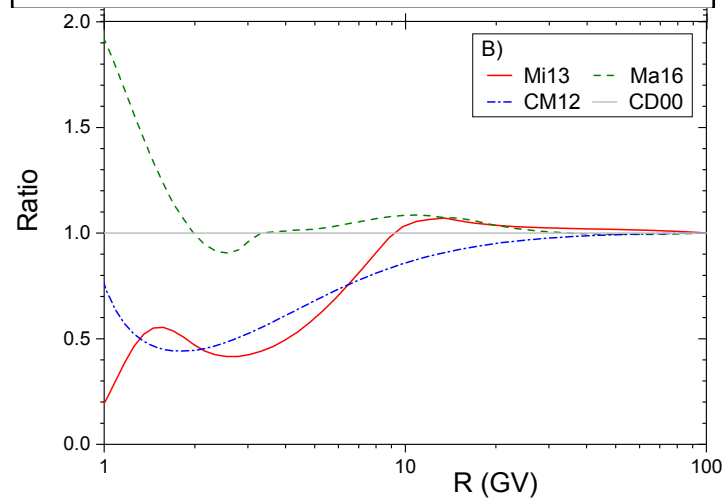
GLE69 (20-Jan-2005)



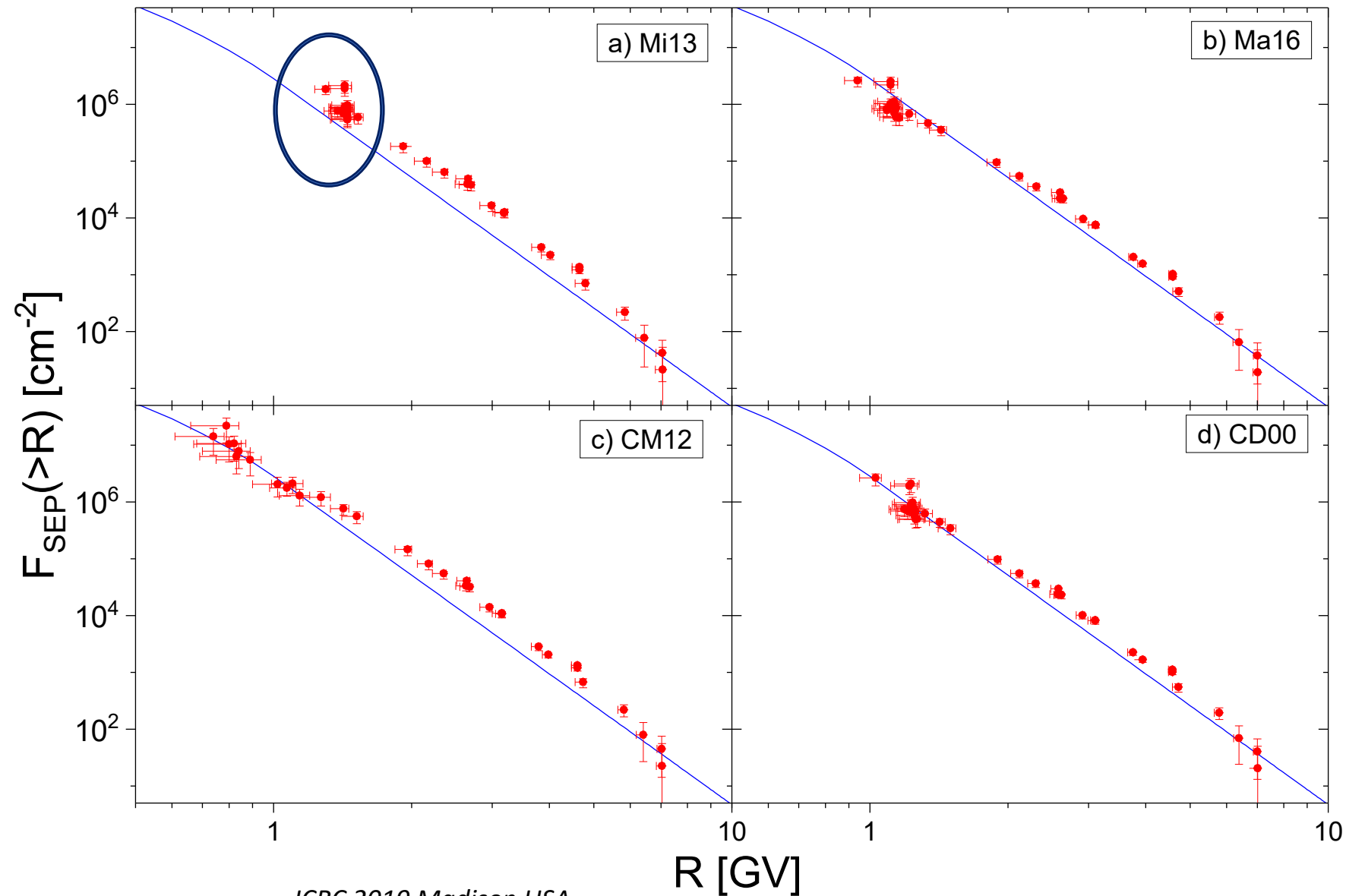
Four modern neutron monitor yield function were tested:

- Mishev et al. 2013
- Caballero-Lopez and Moraal 2012
- Mangeard et al. 2016
- Chem and Dorman 2000

For all these YFs the attitude dependence from FI08 YF was used



GLE69 (20-Jan-2005)



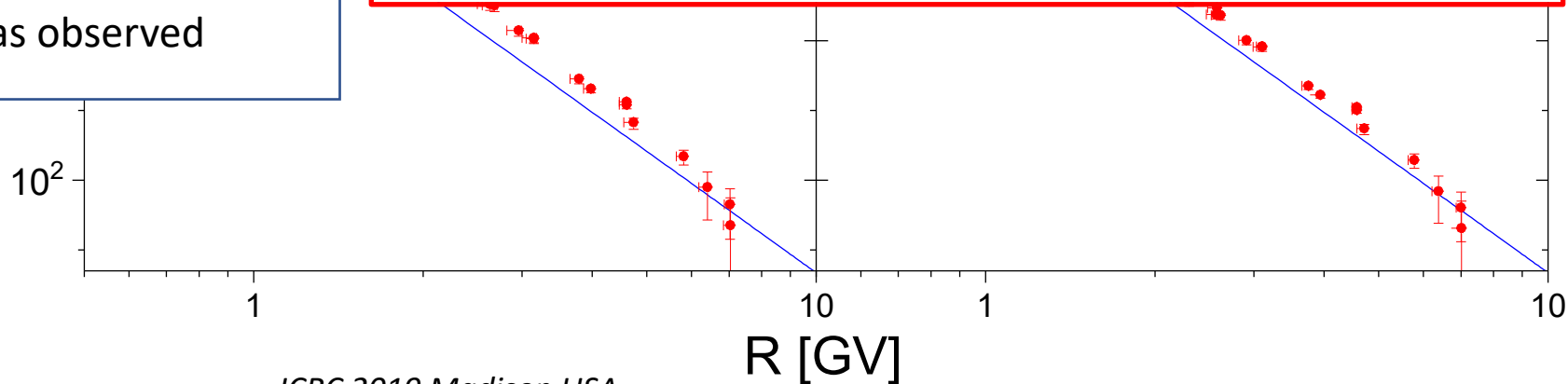
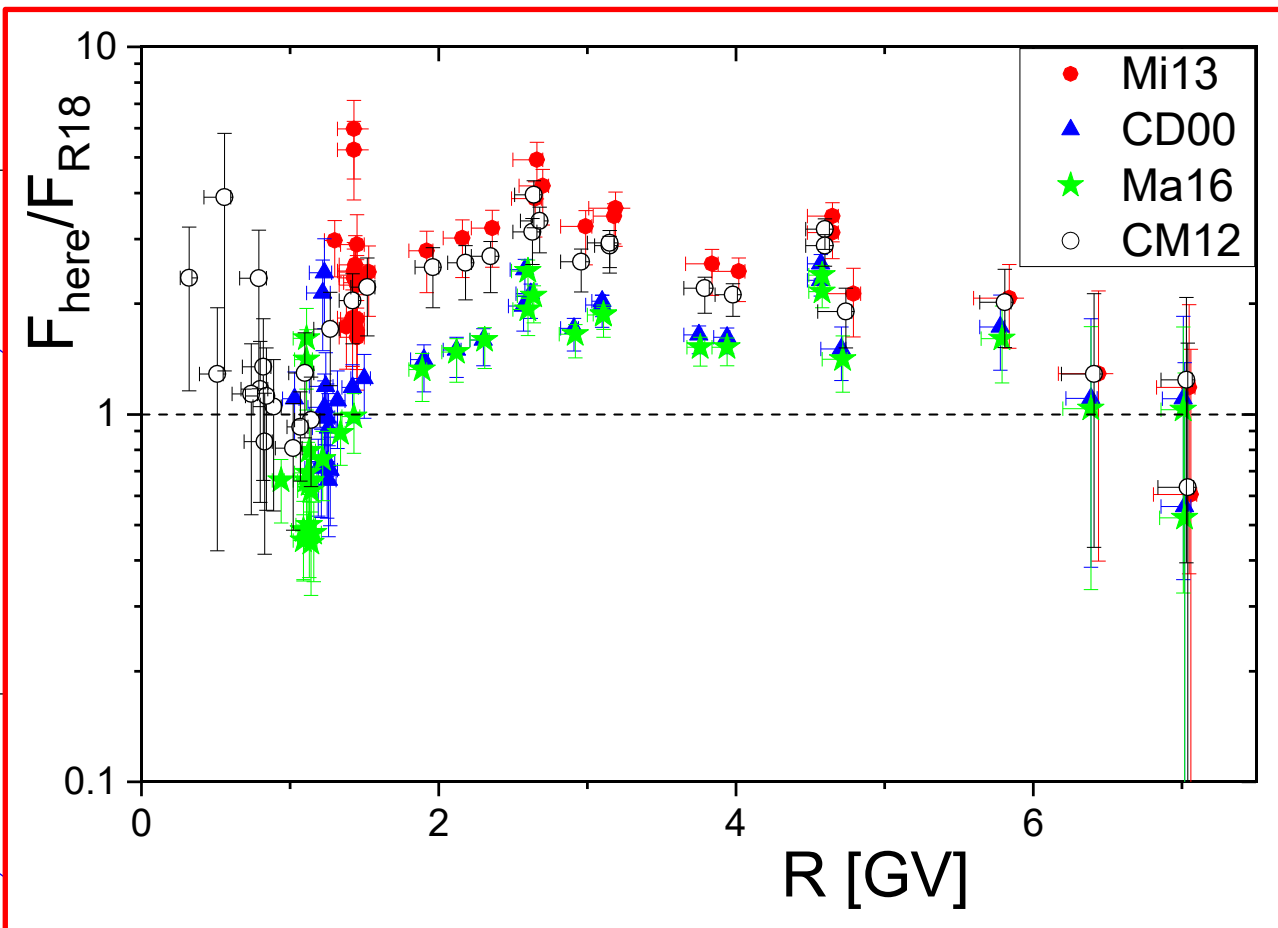
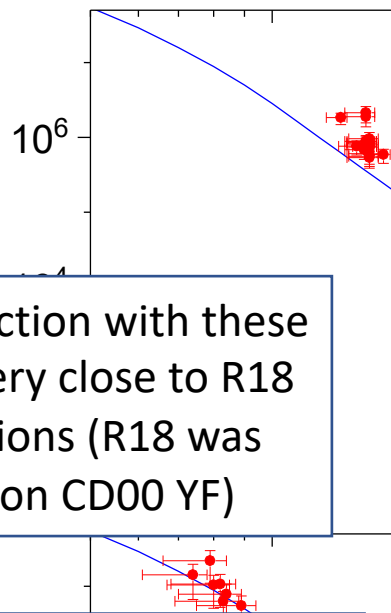
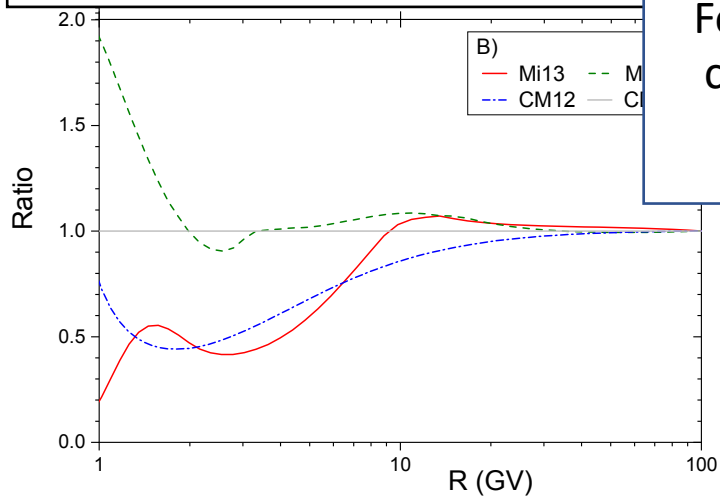
Four modern neutron monitor yield function were tested:

- Mishev et al. 2013
- Caballero-Lopez and Moraal 2012
- Mangeard et al. 2016
- Chem and Dorman 2000

For all these YFs the attitude dependence from FI08 YF was used

Reconstruction with these YFs lies very close to R18 calculations (R18 was based on CD00 YF)

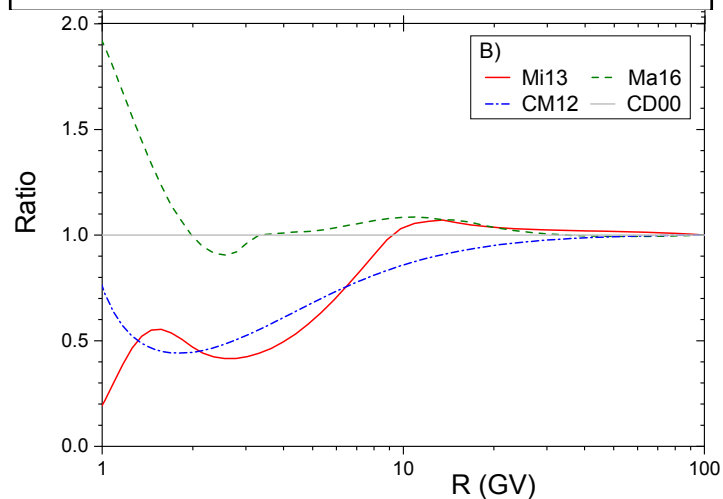
For all YFs some kind of cutoff in high energies was observed



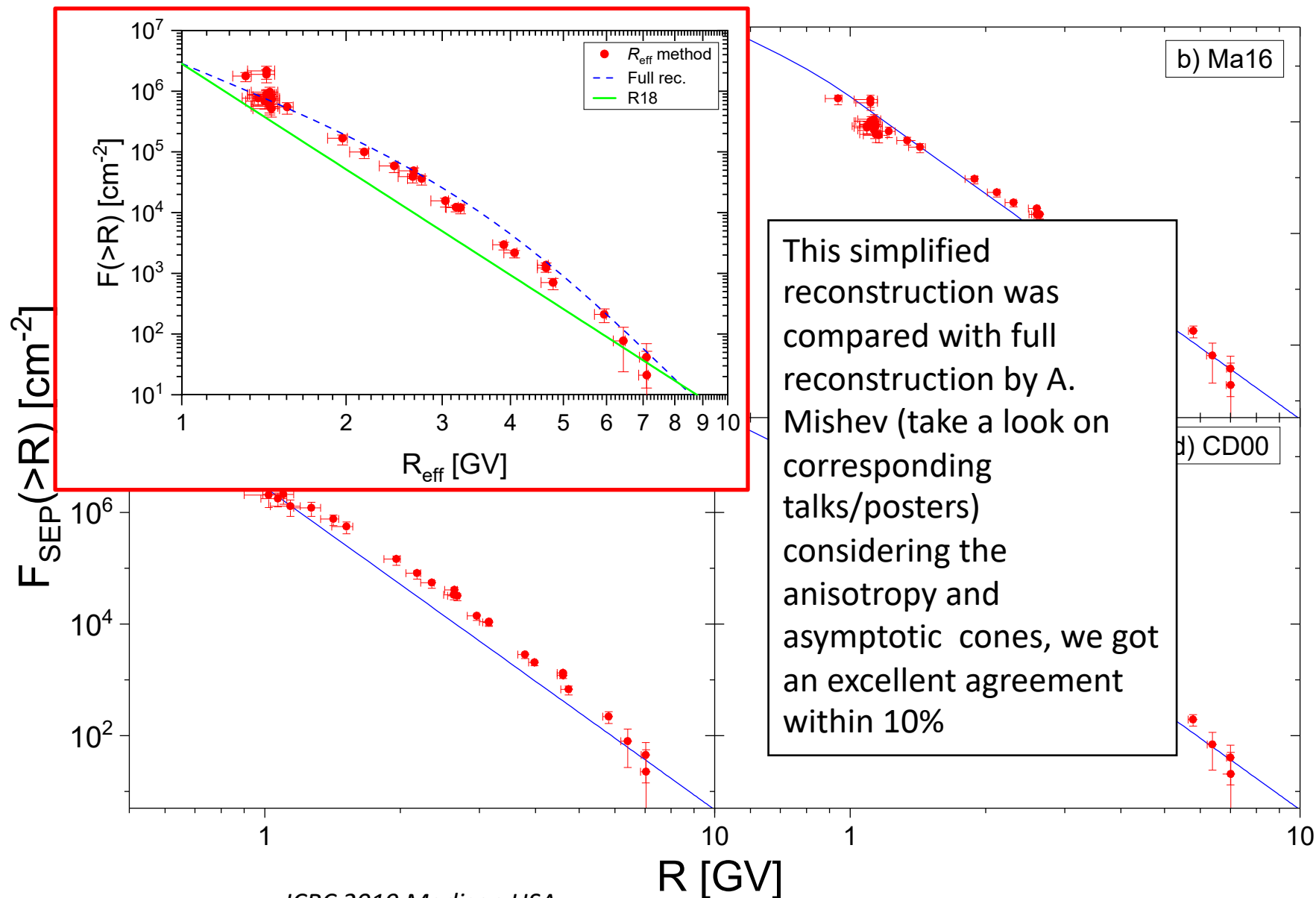
Four modern neutron monitor yield function were tested:

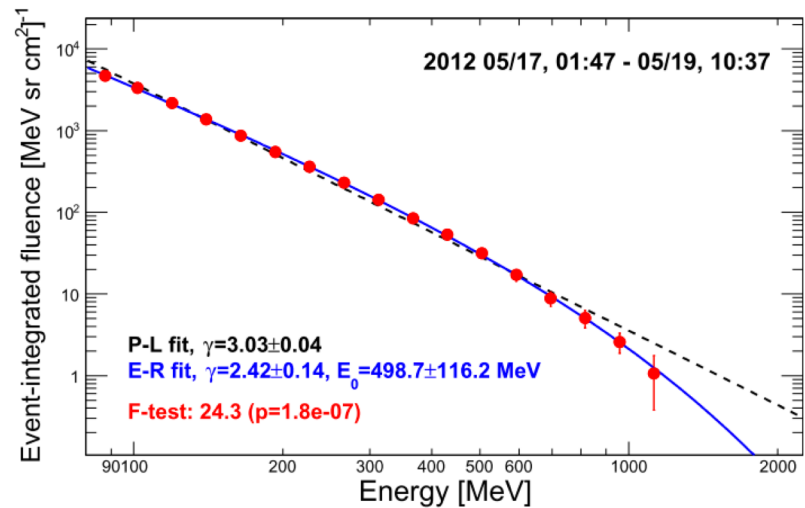
- Mishev et al. 2013
- Caballero-Lopez and Moraal 2012
- Mangeard et al. 2016
- Chem and Dorman 2000

For all these YFs the attitude dependence from FI08 YF was used



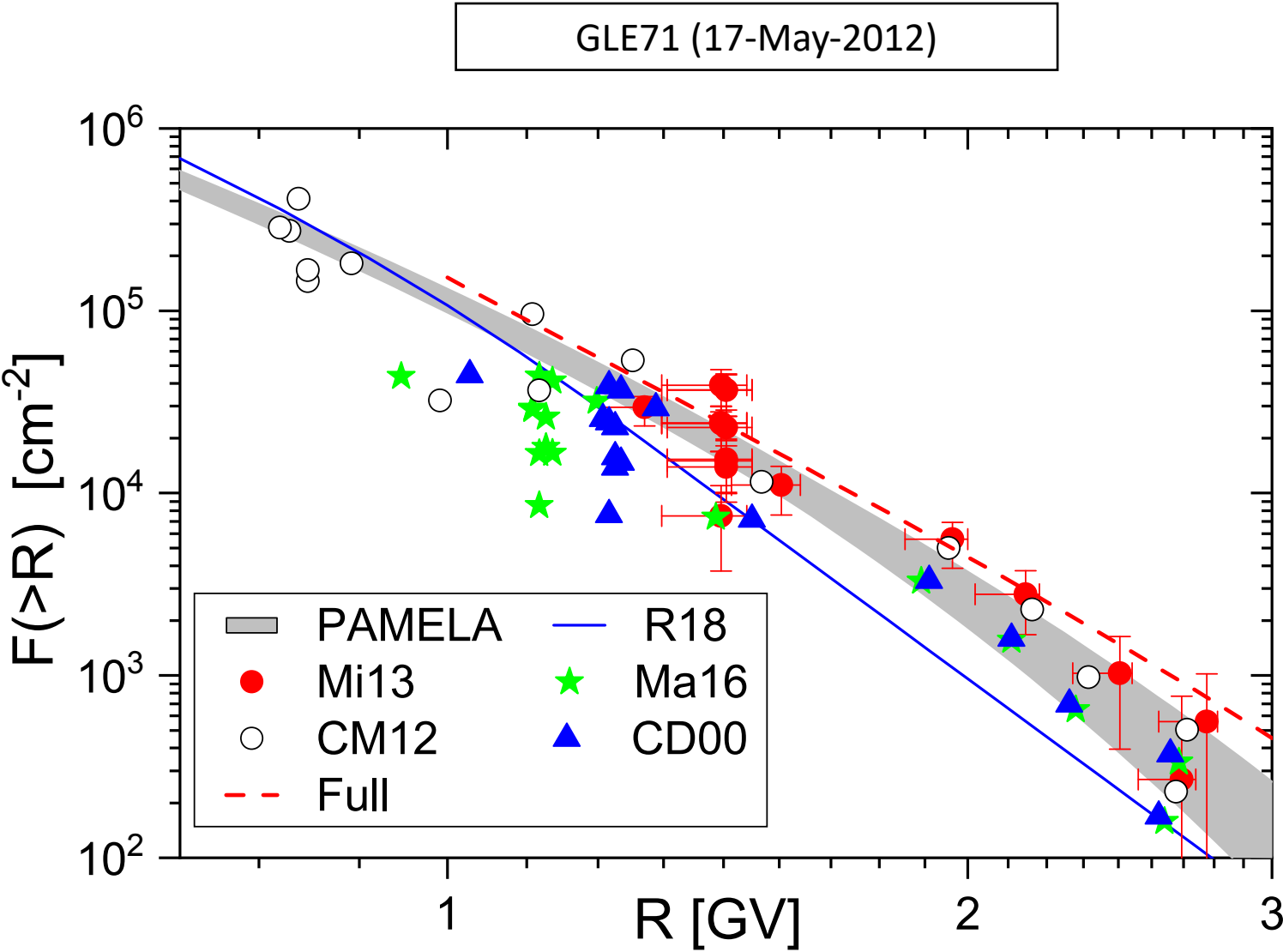
GLE69 (20-Jan-2005)





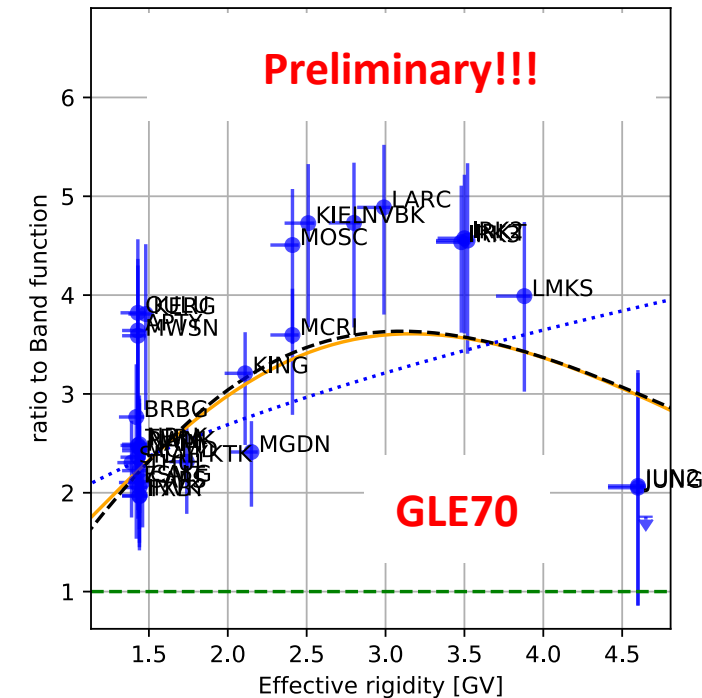
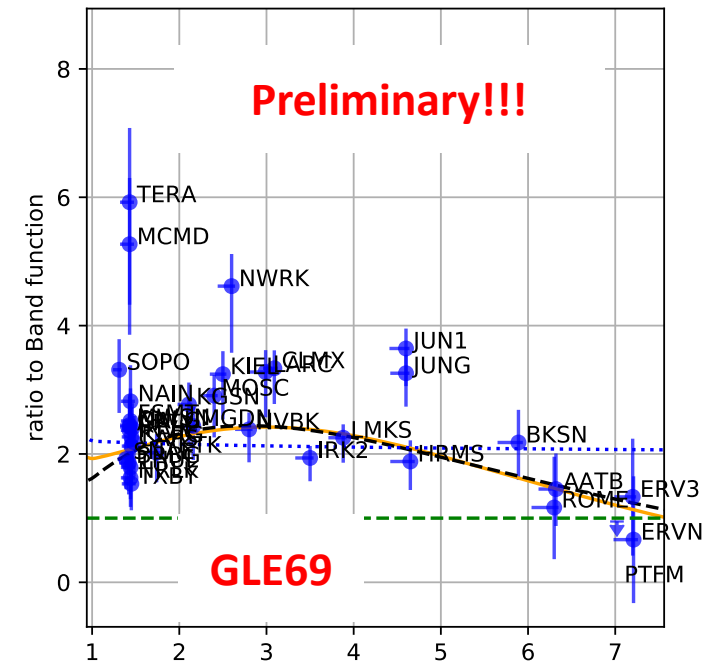
PAMELA direct measurements are in better agreement with CM12 and Mi13 yield function, CD00 and Ma16 YF possibly overestimate the NM response in low-energy region.

This conclusion is in agreement with conclusions of NM YF validation made with use of AMS-02 proton and helium monthly data.



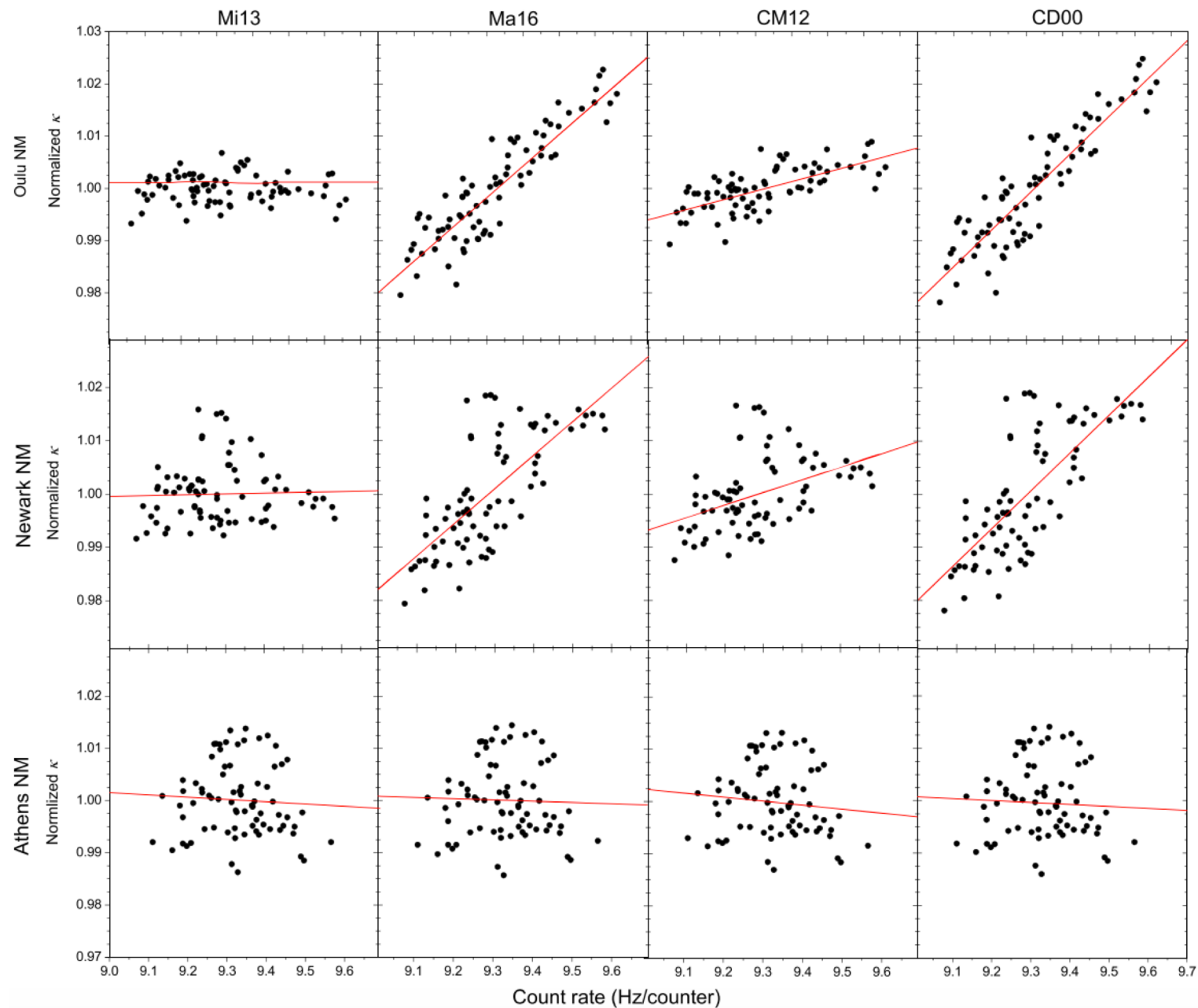
Conclusion

1. The new R_{eff} method of GLE fluence reconstruction is developed, that allows to use the NM as an integral detector and get the coefficient between the neutron monitor count rate and the SEP fluence.
2. GLE #69, 71 were analyzed using the new method. The main feature that obtained results shows good agreement with direct PAMELA measurements for GLE #71 using Mi13 and CM12 yield function, that serves an independent evidence of conclusions, obtained during NM yield function validation using AMS-02 data.
3. Use of CD00 and Ma16 yield function lead to underestimation of fluence in rigidity range <10 GV.
4. For powerful GLEs such as #69 and 70 obtained fluence shows some kind of steeping, which can be approximated using modified power law, power law + exp or Ellison-Ramaty functions.
5. Work in progress, stay tuned!

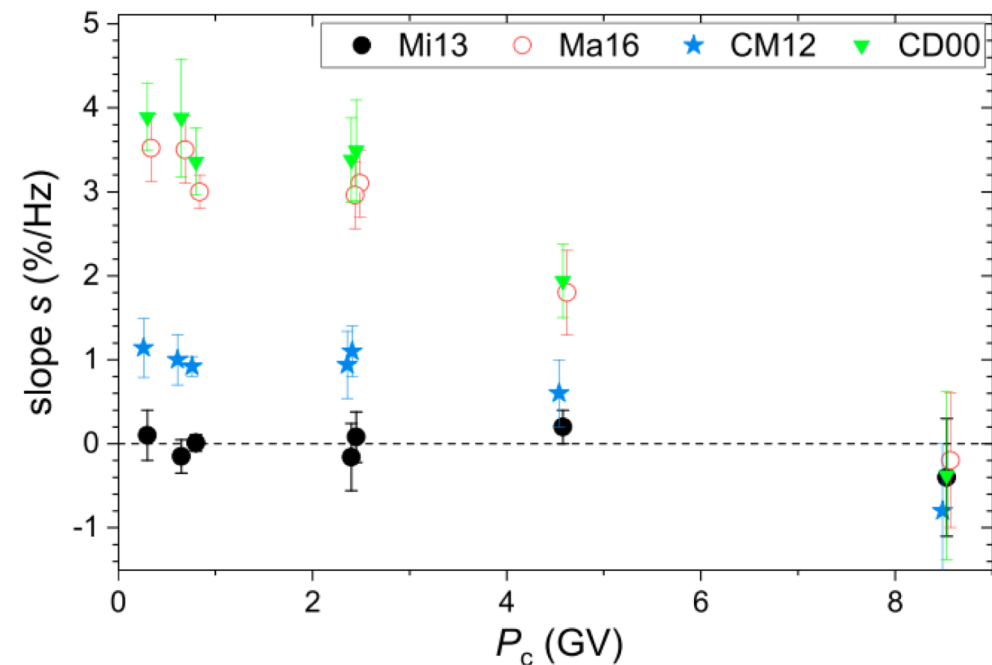


Backup slides

NM calibration with AMS-02 monthly data



JGR:SP (2019) 124(4):2367



The definition of effective rigidity: $F(> R_{eff}) = K_{eff} * N_{GLE}$

Definition of R_{eff} and K_{eff} is the essence of new method

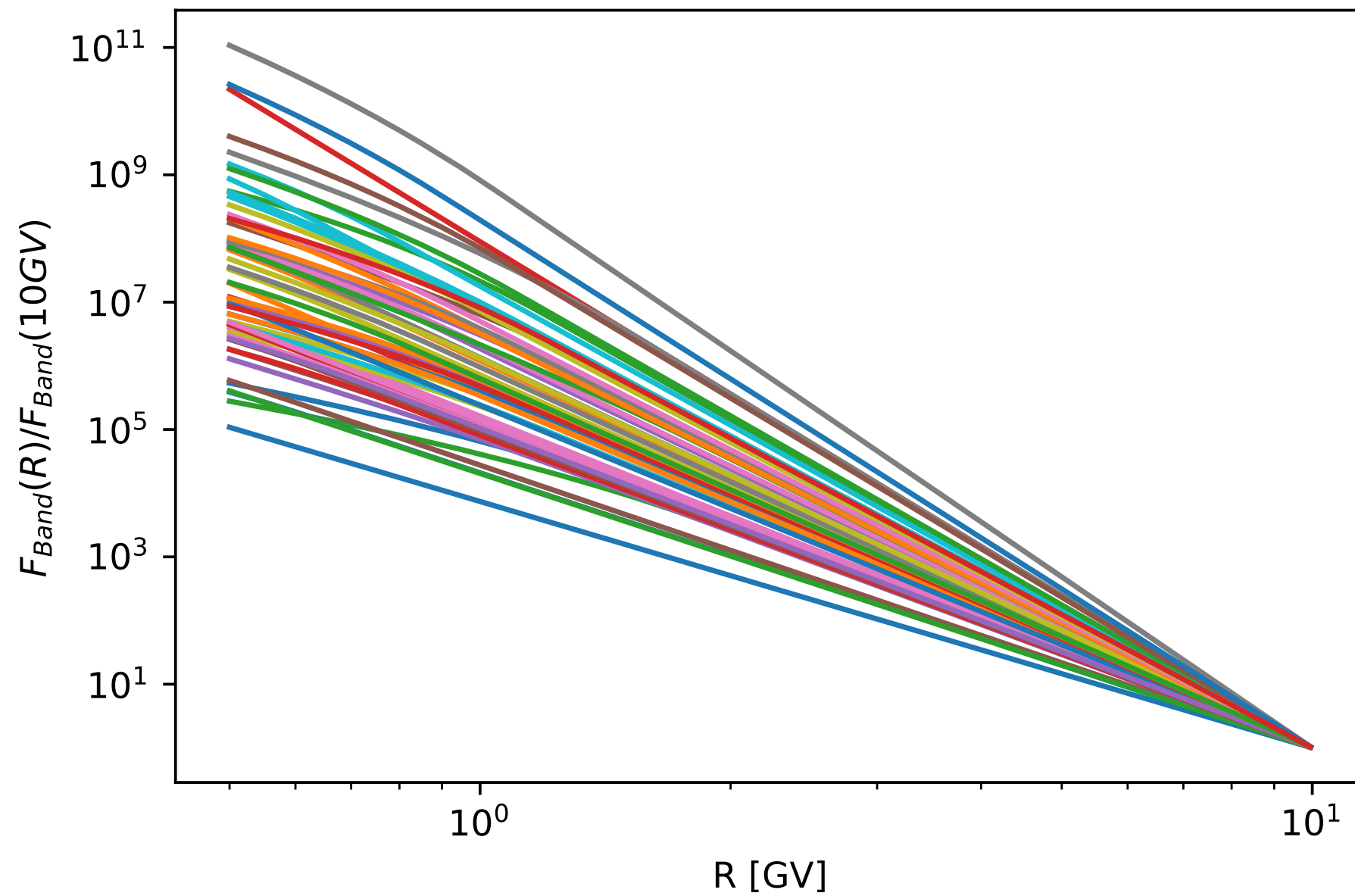
$$N_{GLE} = N_{GCR} * X$$

X is a relative GLE increase in units of [%*hour]

$$N_{GCR} = \sum_i \int_{P_c}^{\infty} J_i(R, t) * Y_i(R, t) dR$$

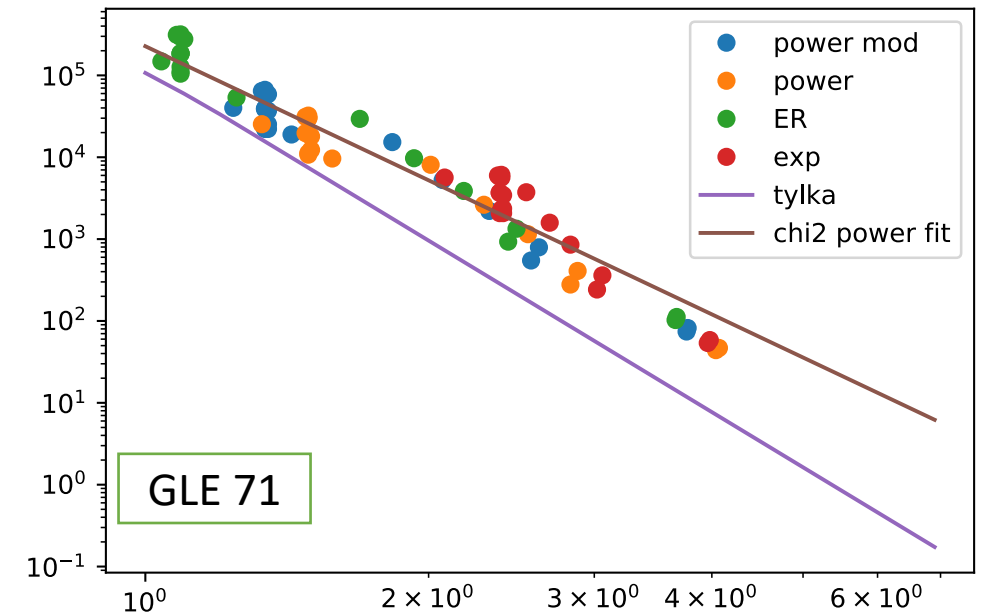
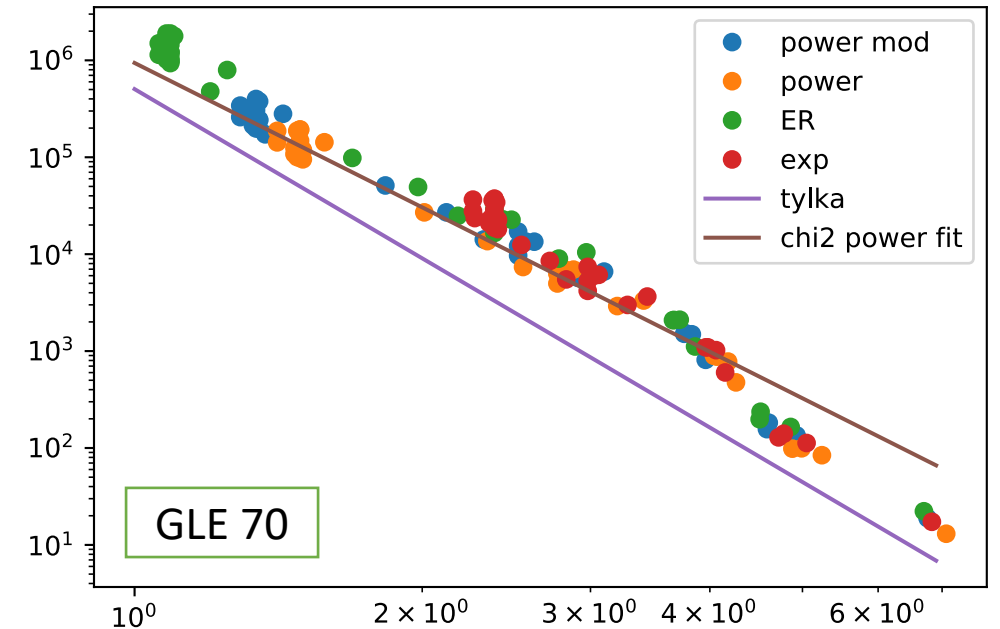
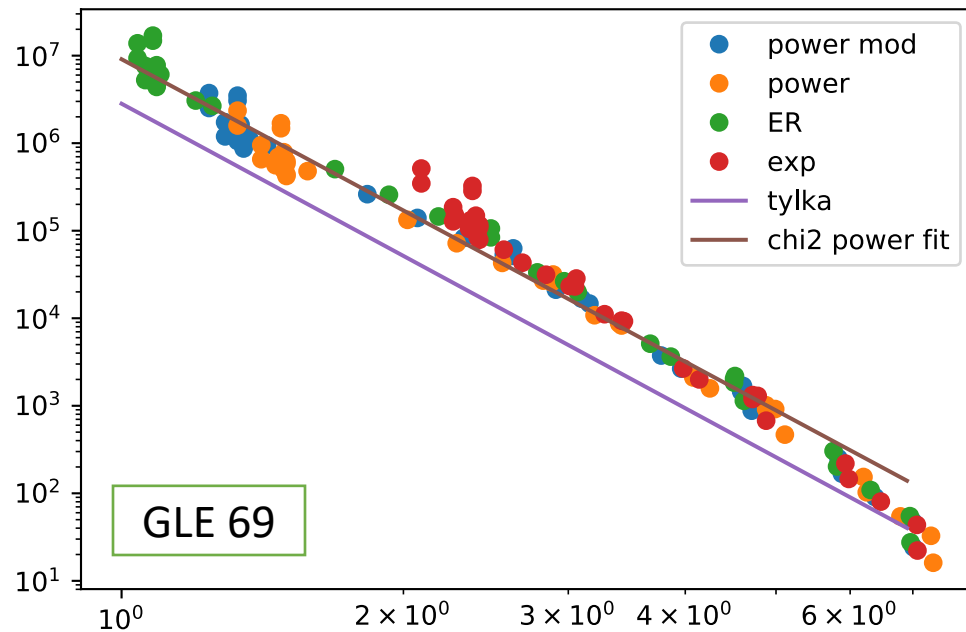
$J_i(R, t)$ is taken as LIS by Vos & Potgieter 2015 modulated using simplified solar modulation potential φ . φ values were taken from Usoskin et al. 2017

LIS of heavy nuclei were taken as proton LIS with ~0.35 coefficient.

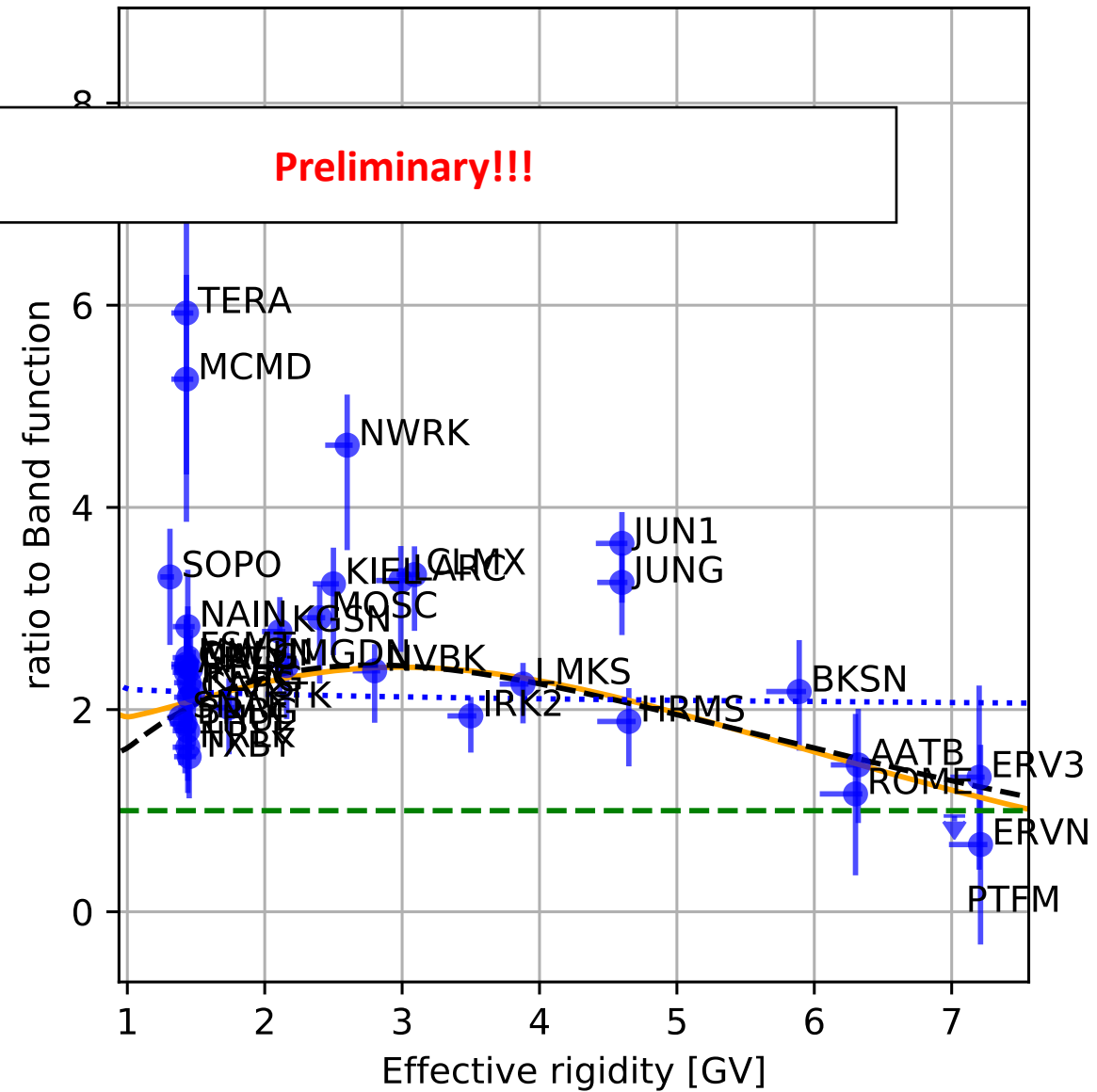
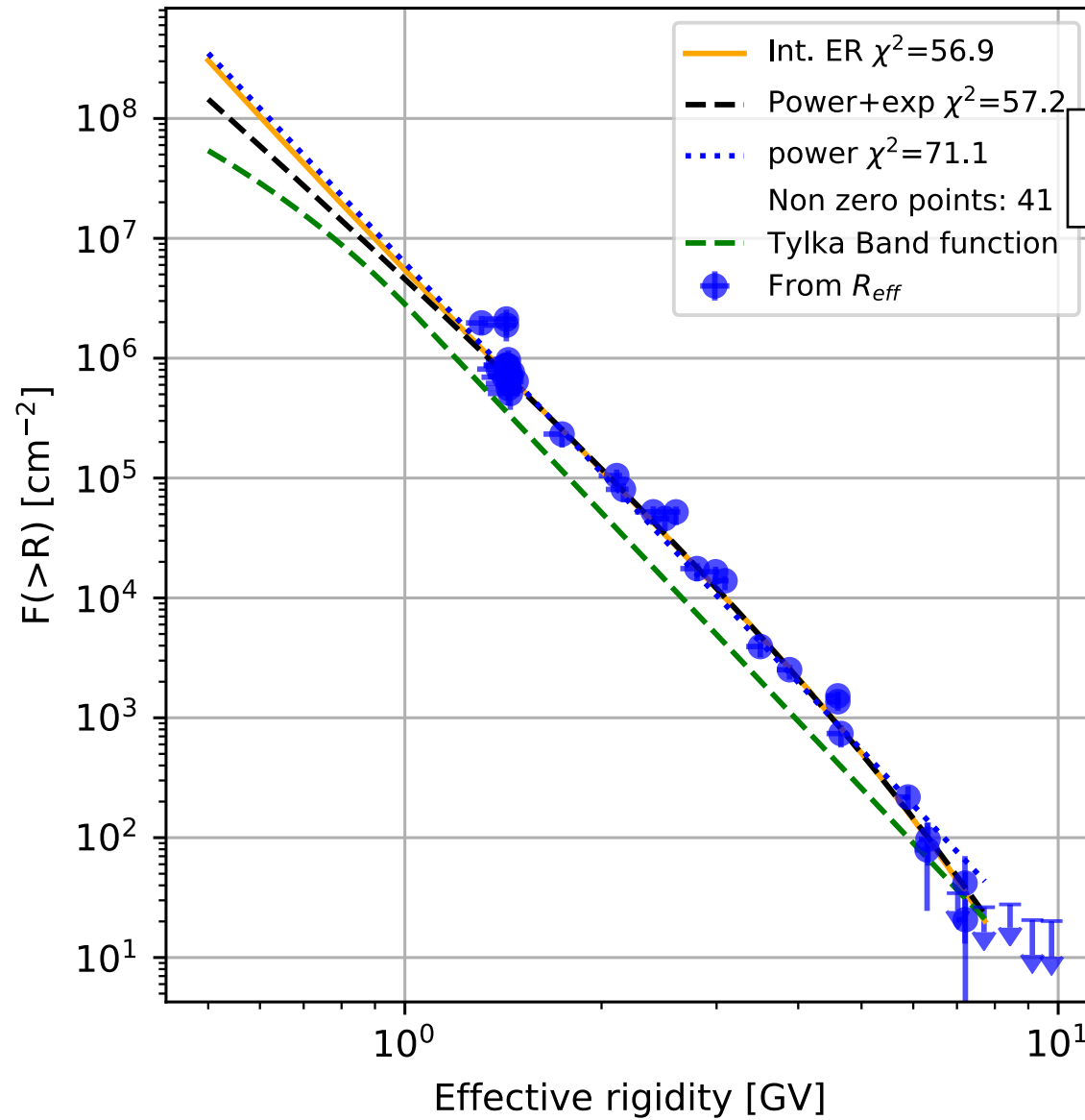


R_{eff} function test

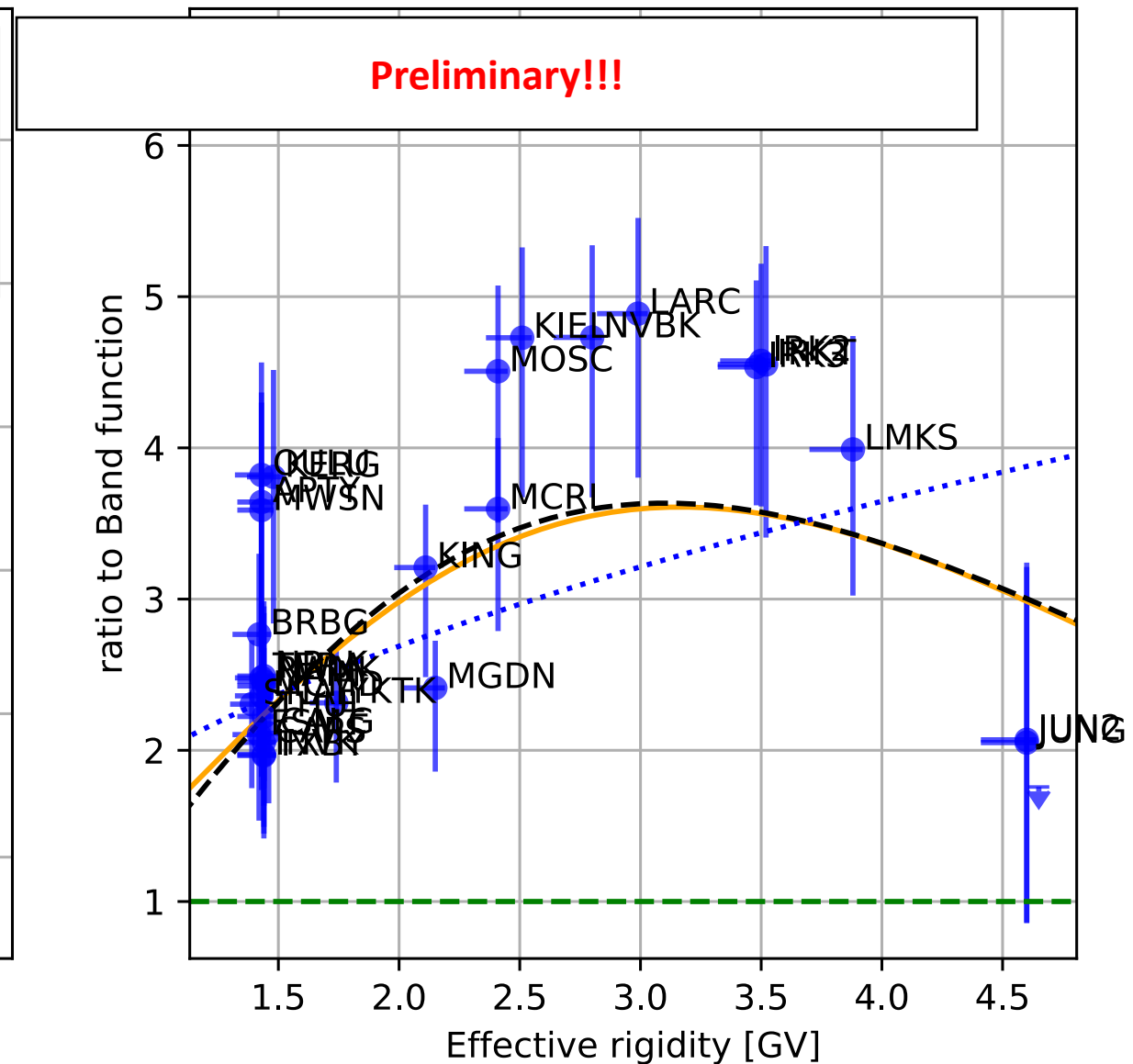
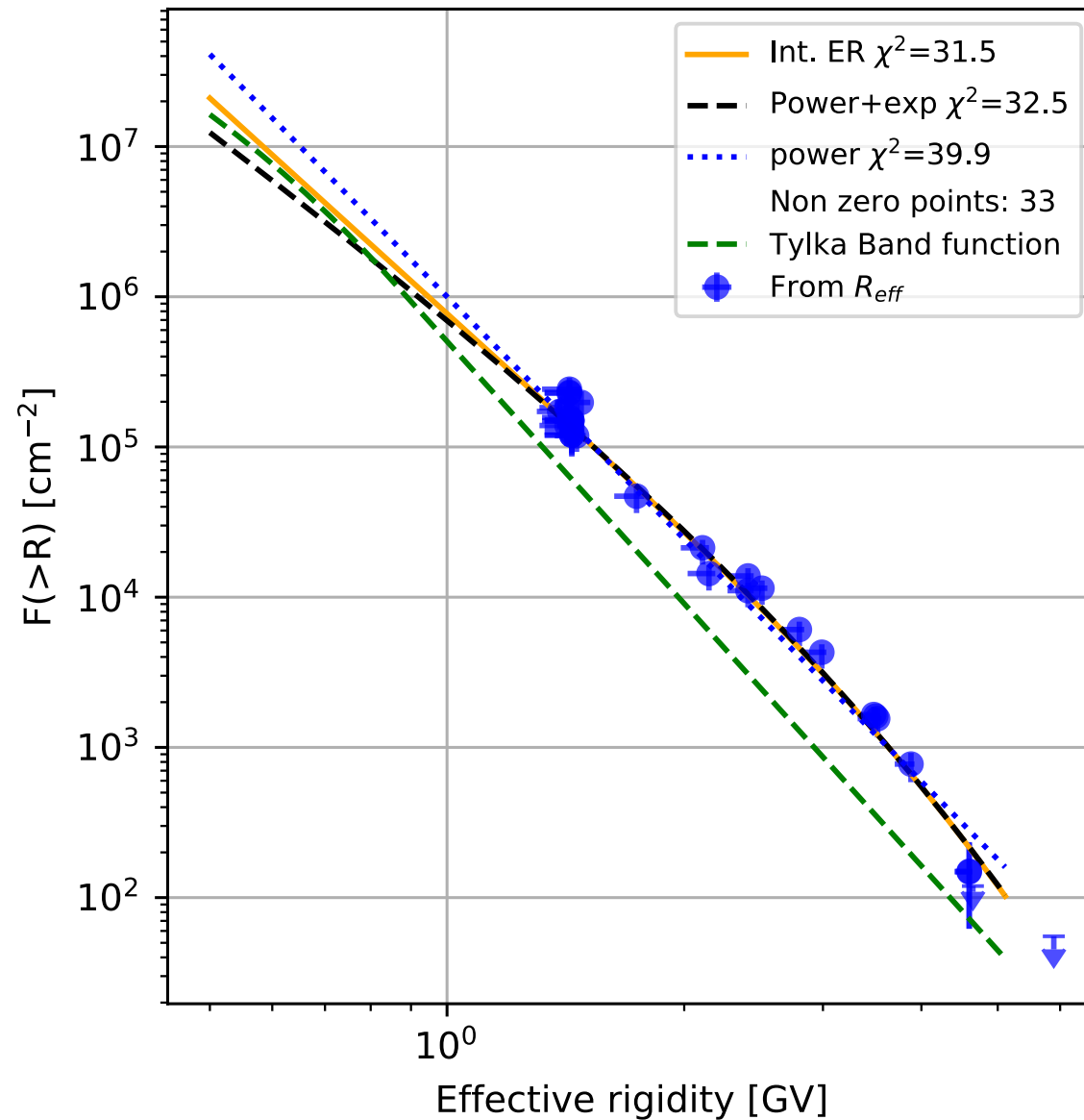
Usage of different as an source function for $R_{\text{eff}}/K_{\text{eff}}$ calculation does not change significantly the results of fluence reconstruction



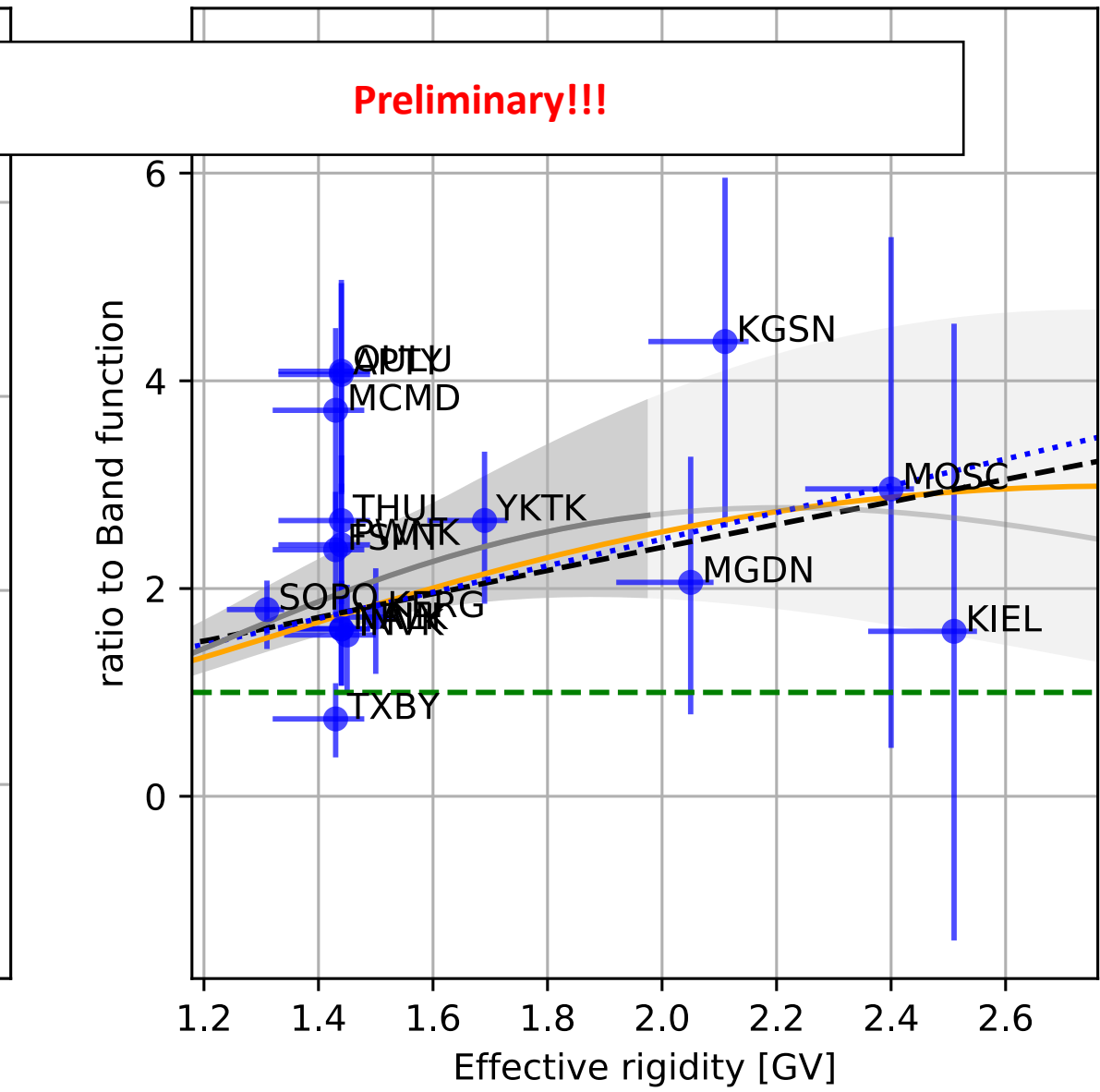
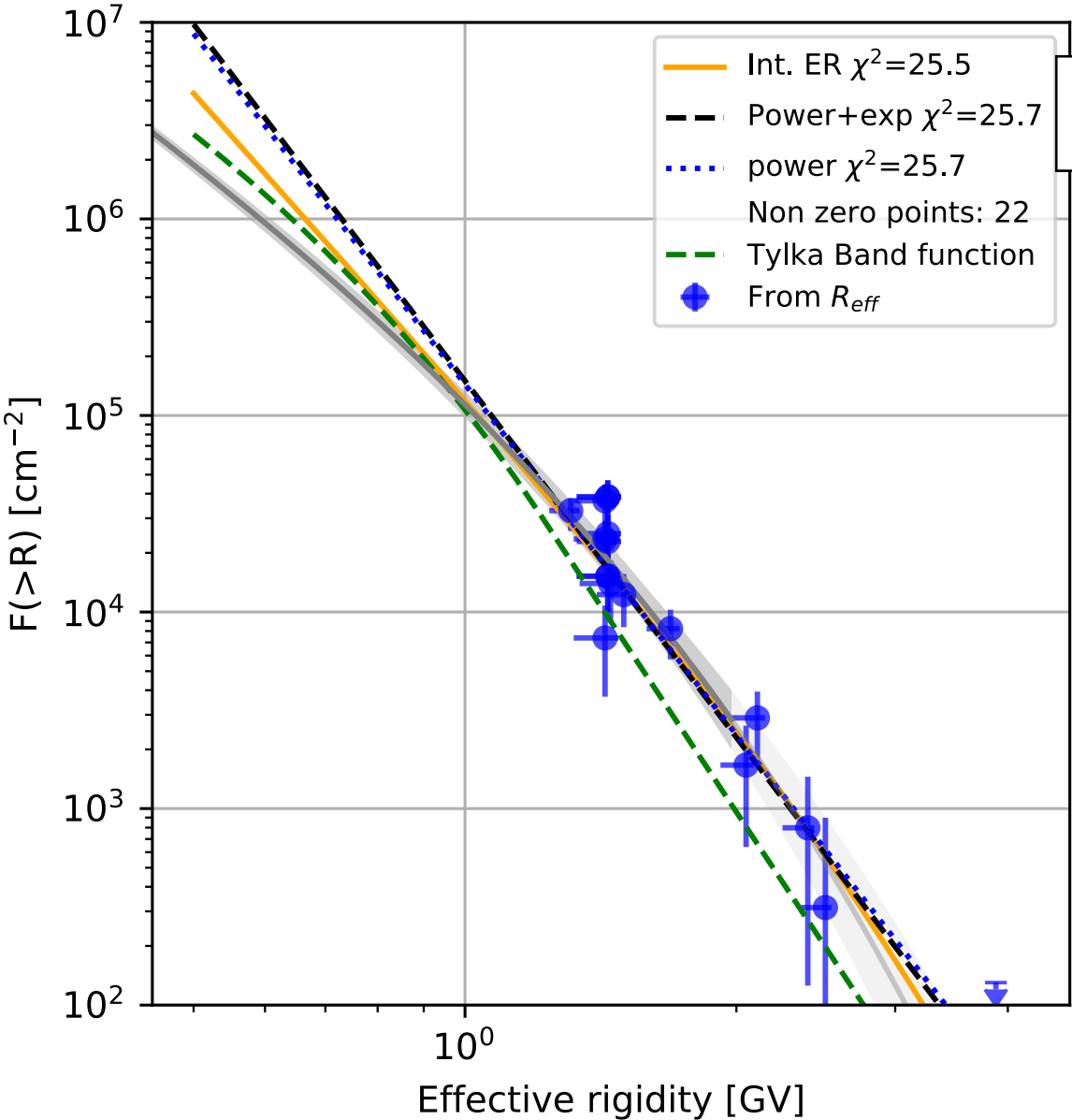
GLE69 // 20 Jan 2005



GLE70 // 13 Dec 2006



GLE71 // 16 May 2012



GLE42 // 29 Sep 1989

